AD_____

Award Number: DAMD17-96-1-6141

TITLE: Characterization of Two Proteins which Interact with the
      BRCA1 Gene

PRINCIPAL INVESTIGATOR: Frank J. Rauscher, Ph.D.

CONTRACTING ORGANIZATION: The Wistar Institute
                          Philadelphia, Pennsylvania   19104-4268

REPORT DATE: June 1999

TYPE OF REPORT: Annual

PREPARED FOR: U.S. Army Medical Research and Materiel Command
                Fort Detrick, Maryland   21702-5012

DISTRIBUTION STATEMENT: Approved for Public Release;
                        Distribution Unlimited

The views, opinions and/or findings contained in this report are
those of the author(s) and should not be construed as an official
Department of the Army position, policy or decision unless so
designated by other documentation.

20000829 033

REPORT DOCUMENTATION PAGE	Form Approved OMB No. 0704-0188

1. AGENCY USE ONLY *(Leave blank)*	2. REPORT DATE June 1999	3. REPORT TYPE AND DATES COVERED Annual (1 Jun 98 – 31 May 99)

4. TITLE AND SUBTITLE
Characterization of Two Proteins which Interact with the BRCA1 Gene

5. FUNDING NUMBERS
DAMD17-96-1-6141

6. AUTHOR(S)
Frank J. Rauscher, Ph.D.

7. PERFORMING ORGANIZATION NAME(S) AND ADDRESS(ES)
The Wistar Institute
Philadelphia, Pennsylvania 19104-4268

8. PERFORMING ORGANIZATION REPORT NUMBER

9. SPONSORING / MONITORING AGENCY NAME(S) AND ADDRESS(ES)
U.S. Army Medical Research and Materiel Command
Fort Detrick, Maryland 21702-5012

10. SPONSORING / MONITORING AGENCY REPORT NUMBER

11. SUPPLEMENTARY NOTES

12a. DISTRIBUTION / AVAILABILITY STATEMENT
Approved for Public Release; Distribution Unlimited

12b. DISTRIBUTION CODE

13. ABSTRACT *(Maximum 200 words)*

We have made extensive progress in the past year to support our analysis of the BAP1-BRCA1 interaction. We have published the co-localization and cell-cycle patterns of intranuclear distribution for the two proteins. In addition, we have shown that BAP-1 is a bonafide tumor suppressor gene which is able to inhibit the malignant growth characteristics of cell lines when transfected back into the BAP1 null cells. This activity is dependent upon enzymatic function of the ubiquitin hydrolysis domain. In exciting preliminary studies we have shown that BAP1, like BRCA1, has a direct role in transcription-coupled DNA repair. The work accomplished conforms to the original SOW and has shed new light on the role of BRCA1 as a tumor suppressor in early onset familial breast-ovarian cancer families.

14. SUBJECT TERMS
Breast Cancer

15. NUMBER OF PAGES 34

16. PRICE CODE

17. SECURITY CLASSIFICATION OF REPORT Unclassified	18. SECURITY CLASSIFICATION OF THIS PAGE Unclassified	19. SECURITY CLASSIFICATION OF ABSTRACT Unclassified	20. LIMITATION OF ABSTRACT Unlimited

FOREWORD

Opinions, interpretations, conclusions and recommendations are those of the author and are not necessarily endorsed by the U.S. Army.

✓ Where copyrighted material is quoted, permission has been obtained to use such material.

✓ Where material from documents designated for limited distribution is quoted, permission has been obtained to use the material.

✓ Citations of commercial organizations and trade names in this report do not constitute an official Department of Army endorsement or approval of the products or services of these organizations.

✓ In conducting research using animals, the investigator(s) adhered to the "Guide for the Care and Use of Laboratory Animals," prepared by the Committee on Care and Use of Laboratory Animals of the Institute of Laboratory Resources, National Research Council (NIH Publication No. 86-23, Revised 1985).

✓ For the protection of human subjects, the investigator(s) adhered to policies of applicable Federal Law 45 CFR 46.

✓ In conducting research utilizing recombinant DNA technology, the investigator(s) adhered to current guidelines promulgated by the National Institutes of Health.

✓ In the conduct of research utilizing recombinant DNA, the investigator(s) adhered to the NIH Guidelines for Research Involving Recombinant DNA Molecules.

✓ In the conduct of research involving hazardous organisms, the investigator(s) adhered to the CDC-NIH Guide for Biosafety in Microbiological and Biomedical Laboratories.

PI - Signature   2/17/90   Date

CHARACTERIZATION OF TWO PROTEINS WHICH INTERACT WITH THE BRCA1 GENE

TABLE OF CONTENTS

Introduction

      We have previously identified a novel protein, BAP1 (BRCA1 Associated Protein-1), which binds to the wild-type, but not to a mutated, BRCA1 RING finger domain (1). BAP1 is a novel, nuclear-localized member of the ubiquitin carboxy-terminal hydrolase (UCH) family of enzymes (reviewed in (2, 3)). BAP1 is a 729 a.a. protein (90 kDa apparent molecular weight) that binds to BRCA1 *in vitro* and *in vivo* , cleaves ubiquitin from a model substrate, is co-expressed temporally and spatially with BRCA1 and enhances the growth suppressive properties of BRCA1

      Through its association with BRCA1, BAP1 is also indirectly implicated in DNA repair processes. For example, BRCA1 and p53 have been shown to associate (4), and it is known that p53 protein levels are regulated through the ubiquitin/proteasome pathway (5). Thus, BAP1, BRCA1, and p53 might possibly exist (albeit transiently) within the same complex and may crucially determine control of the cells' response to DNA damage. This linkage of BAP1 to cellular DNA repair processes is further supported by the association of BRCA1 (6) {and BRCA2 (7)} with the RAD51 protein and by the recent findings that BRCA1 null cells are deficient in transcription-coupled DNA repair (8, 9). The RAD51/52-dependent DNA repair pathway is highly regulated and contains many proteins which may be potential substrates for BAP1-mediated ubiquitin hydrolysis. Furthermore, the RAD51/52 complex was recently shown to contain both an ubiquitin-like protein, UBL-1 (10, 11) and a ubiquitin-like conjugating enzyme, hUBC9/UBE2I (12). Thus, the BRCA1/BRCA2-RAD51 DNA repair complex contains the elements necessary to conjugate an ubiquitin-like molecule to proteins of the complex BRCA1, and suggests the possibility that BAP1 might be a part of this ubiquitin-like pathway.

      BAP1's potential importance in genomic stability and integrity was further signaled by the mapping of the human *BAP1* locus to chromosome 3p21.3 (1), a region of the genome that is routinely deleted or rearranged in many cancers. We have found rearrangements, deletions and missense mutations of *BAP1* in small cell and non-small cell lung cancer cell lines and, more recently, in breast cancer tumor samples (manuscript in preparation). These data suggest that *BAP1* may be a tumor suppressor gene. In this past year of support we have investigated this possibility by transfecting BAP1 or an enzymatically inactive form of BAP1 into the non-small cell lung cancer cell line NCI-H226, a cell line lacking endogenous BAP1 (1). Our results show that wild-type BAP1 decreases cell growth, changes cell shape and inhibits *in vivo* tumor growth. We have also determined the role of BAP1 in BRCA1 mediated DNA repair processes.

Body

I.   Materials and Methods

Cell Culture and Stable Cell Lines: All cells were maintained at 37°C and 5% CO_2. NCI-H226 cells and all subclones were grown in RPMI1640 (Mediatech) containing 10% FBS (Hyclone). The NCI-H226 cell line has previously been shown to lack BAP1 expression due to a rearrangement of chromosome 3 at the BAP1 gene (jensen et al.). NCI-H226 cell lines (over)expressing BAP1 or BAP1(C91S) were generated by transfection via Ca-phosphate precipitation (Chen and Okayama MCB 1987). Cells were transfected with vector alone (pcDNA3; Invitrogen), the BAP1 cDNA or the BAP1(C91S) cDNA. After 24 hours of recovery, the cells were placed in RPMI1640 +10% FBS containing 0.2 mg/mL G418 (Mediatech). Cells were fed fresh medium twice per week and colonies were selected 21 days later. Subclones were screened for BAP1 or BAP1(C91S) protein expression by Western analysis using the 3C11 monoclonal antibody.

Cell Growth Assays: Cells were plated (in medium containing 2% FCS) to 24-well plates (Falcon) at $5X10^3$ cells per well. Daily determinations of cell growth were performed by adding 1/10 volume of MTT solution (5 mg/mL in phosphate-buffered saline) to one well of each cell line. The cells were incubated for exactly one hour, the medium siphoned off and the cells lysed by the addition of 1 mL of DMSO. This solution was analyzed by reading its O.D. at 550 nm.

SCID Mice: Tumorigenesis assays were carried out in CB17 SCID mice that were obtained from the Wistar Institute's in-house animal facility. Tumors were initiated by the s.c. injection of $5X10^6$ cells per mouse. After a period of 4-5 weeks, mice were sacrificed and the tumors excised and measured. Each tumor was then subdivided into several pieces for analysis.

Monoclonal antibody production: The human BAP1 cDNA was fused (inframe) downstream of the 6 Histidine residues of the vector pQE-30 (QIAGEN Inc.). The His-tagged protein was purified from *E.coli* over a Ni-agarose column as previously described (20). 50 μg recombinant 6XHis-BAP1 fusion protein, in 50 μl PBS, was emulsified in complete Freund' adjuvant and injected s.c. into Balb/c mice followed by 3 boosts in incomplete Freund adjuvant. The 4th boost was given i.v. and the splenocytes were fused three days later with the mouse non-Ig secreting cell line P3X63Ag8.SP2/0. Hybridomas were selected by testing supernatants by Elisa on several recombinant GST fusion proteins: GST-BAP1(aa 1-250), GST-BAP1 (aa 300-480???) and GST-BAP1(aa 494-729). Clones that reacted with one fusion protein but not the other two were selected, subcloned, and retested for reactivity. A subset of

these clones were then developed further. All resulting monoclonal antibodies were of the IgG1, kappa subtype.

Immunoprecipitation: The Promega TNT kit was used as described by the manufacturer to produce ^{35}S-labeled BAP1 protein. Protein was used for analysis without further purification. Immunoprecipitations were carried out by incubating the antibody with *in vitro*-produced protein in 1 mL of RIPA buffer for 2 hours at 4°C. Protein G sepharose resin (Pharmacia) was added and incubated for a further 30-45 mins. at 4°C with continual mixing. The bound proteins were washed in RIPA buffer 4 times, released from the sepharose resin with SDS-PAGE loading dye and separated by SDS-PAGE. Visualization of bound protein was performed by fluorography.

Western Blot Analysis: Cell lines were lysed directly in loading buffer (100 mM TRIS, ph 6.8, 4% SDS, 20% glycerol). Tissue samples were sonicated in loading buffer (5 pulses, 50% output) and then centrifuged at 15,000 X g for 20 minutes at 4°C. The supernatant was then collected and processed further. Samples were heated at 100°C for 10 minutes, cooled, and then the protein concentration was determined (Bradford, bird). Finally, DTT was added to the samples to a final concentration of 50 mM and the samples were reheated at 100°C for 2 minutes. Proteins were separated by SDS-PAGE and transferred to PVDF membrane (Millipore) via standard methods. The membrane was then blocked in Tris-buffered Saline containing 0.1% Tween-20 (TBST) and 5% fish gelatin (Forma Scientific). The mAb 3C11 hybridoma supernatant was diluted 1:5 into the block buffer and incubated with the membrane for 2 hours at room temperature with gentle shaking. After washing the membrane 3 times with TBST (10 minutes each), the blot was incubated with secondary antibody conjugated to horse radish peroxidase (goat anti-mouse IgG-HRP; BioRad) at 1:5000 dilution for 30 minutes. The membrane was washed 3 times further and developed with Super Signal (Pierce).

II. Results and Discussion

Expression of BAP1 in the NCI-H226 non-small cell lung cancer cell line.

In our report had suggested that BAP1 may have growth/tumor suppressive properties beyond its enhancement of BRCA1-mediated growth suppression (1). That report also identified a cell line, the NCI-H226 non-small cell lung cancer cell line (H226 cells), that did not express BAP1 mRNA or protein (1). This cell line would then provide an extremely useful tool in which to characterize the possible growth and/or tumor suppressive effects of BAP1.

Another necessary tool for these analyses was a high affinity, and highly specific, antibody directed against BAP1. Monoclonal antibodies with epitopes directed to different regions of BAP1 (Figure 1A) were prepared and characterized. Immunoprecipitation analysis of ^{35}S-labeled *in vitro* transcribed and translated BAP1 protein showed that each of the antibodies detected BAP1 with the 3C11 isolate showing the strongest reactivity of the three monoclonal antibodies (Figure 1B). Western analysis showed that BAP1 was expressed in several cell lines at similar levels (Figure 1C). Since the monoclonal isolate 3C11 delivered the strongest signal in these

assays (the polyclonal antibody does not appear to work in Western analysis) it was routinely used throughout the experiments described below.

Cell lines expressing wild-type BAP1 (BAP1), mutant BAP1 [the enzymatically inactive BAP1(C91S)] or containing the expression vector pcDNA3 alone (vector) were generated by Ca^{+2}-phosphated-mediated transfection of the H226 cell line. After selection of clones positive for growth in 0.2 mg/mL G418, cell lines expressing both high and low levels of BAP1 or BAP1(C91S) (Figure 1D) were selected and assayed for changes in cell morphology, cell growth rate, anchorage-independent growth and *in vivo* tumorigenesis.

Expression of BAP1 reduces the growth rate of NCI-H226 cells.

Initial experiments performed in our standard growth medium (RPMI + 10% FCS) showed no differences in the growth rates between any of the cell lines (data not shown). However, when the concentration of growth factors was decreased five-fold (i.e. 2% FCS), differences in the growth rates of the individual cell lines became apparent (Figure 2B). The cell lines expressing a higher level of wild-type BAP1 grew at a slower rate compared with the vector cell lines, while cell lines expressing lower levels of BAP1 grew at a rate similar to the vector lines. This same general pattern was also seen with the BAP1(C91S) cell lines suggesting that the level of BAP1 protein in the cell was important to its effects on cell growth. Furthermore, the BAP1 cell lines generally grew slower than the BAP1(C91S) cell lines, suggesting that the enzymatic activity of BAP1 is important in mediating cell growth.

BAP1 expression induces changes in the morphology of NCI-H226 cells.

Expression of BAP1 in the H226 cells gave rise to clones that differed in their appearance (as grown on plastic tissue culture dishes) when compared to all other H226 cell lines. The vector, BAP1(C91S), and the "low expressing" wild-type BAP1 cell lines all had the same appearance, being generally cubical in shape, with nuclei off-center, and growing in tightly packed colonies when plated thinly (Figure 3, top row). In contrast, cells expressing high levels of BAP1 were round in shape, with the nucleus centered within the cell, and growing in patches; The cells touched each other but did not pack together. These characteristics remained even after these cells reached confluence. None of the cells noticeably "piled-up" when over-grown for extended periods of time (up to 4 weeks; data not shown).

BAP1 expression does not affect anchorage-independent cell growth.

The change in morphology of the H226 cell upon expression of BAP1 prompted an investigation into BAP1's effect on anchorage-independent cell growth. All cell lines grew slowly on soft agar, with the parental, vector, and BAP1 cell lines showing no difference in the size of their colonies or their ability to form colonies (Figure 3, bottom row, and data not shown). However, the BAP1(C91S) cell line showed slightly larger colonies after the same period of growth, suggesting that loss of BAP1's enzymatic activity may be important in the progression to a more motile cell state.

5

BAP1 expression in NCI-H226 cells suppresses tumor formation in SCID mice.

To determine whether the expression of BAP1 would affect the tumorigenicity of the NCI-H226 cells, CB17 SCID mice were injected with 5 distinct cell lines over two experiments. The first experiment involved only the comparison of vector and wild-type BAP1 (Table 1). Five mice were each injected with 5×10^6 cells of each cell line. All mice had tumors by the end of the experiment (42 days), however, the tumors from the BAP1 mice were significantly smaller than those from the vector mice, and the mice injected with vector cells had palpable tumors earlier (data not shown). After excision, tumors were assayed for the expression of BAP1 by Western analysis. The tumors derived from cells expressing BAP1 were no longer expressing the BAP1 protein (Figure 4A), suggesting either that these cells had lost their ability to express BAP1 or that a contaminating sub-population of cells which were not expressing BAP1 had grown out during the experiment.

To confirm and expand these results, a second experiment was performed in which vector and BAP1 cell lines, distinct from those of experiment 1, were injected into SCID mice. A BAP1(C91S) cell line was included in this experiment to determine the effect of the loss of BAP1's enzymatic activity on tumorigenicity (Table 1). Mice injected with cells expressing BAP1 developed no tumors while those mice injected with cells expressing vector or BAP1(C91S) developed tumors of the same size and at about the same rate. Tumors derived from cells expressing BAP1(C91S) continued to express this protein as determined by Western analysis (Figure 4B). Although the time period for this experiment was shorter than the previous experiment (30 days vs. 42 days), any developing tumors should have been detected at this point since tumors were detectable at this point in all mice of experiment 1.

Thus, this work accomplished in past year of DoD funding has firmly established that BAP1 is a tumor suppressor gene. Cell lines which lack BAP1 show a highly transformed morphology and grow aggressively in both anchorage independent growth models and in tumor xenografts *in vivo*. However, re-introduction of wild type BAP1 into these cells reverses and/or suppresses the malignant phenotype. Moreover, tumors in mice which do grow after long latencies have either deleted or inactivated expression of the BAP1 transgene, consistent with a tumor suppressor role. Most interestingly, the tumor suppressor function of BAP1 is absolutely dependent on its ubiquitin hydrolase enzymatic activity as a point mutation which changes the catalytic cysteine, no longer functions as a growth suppressor. These findings are the first to implicate a ubiquitin hydrolysis enzyme in cellular growth control. Furthermore, our findings strongly suggest that the VCH enzymatic domain of BAP1 should be a target for mutation in primary human tumor specimens. As part of the original SOW, we are at present searching for such mutations using PCR and SSCP taking advantage of the known genomic structure of human BAP1 which we have solved (in preparation).

Conclusions

1.   We have published a complete characterization of BRCA-1 antibodies (see appendices) and documented the cell-cycle distribution of BRCA1 in the nucleus.

2.   We have demonstrated that BAP1 is a bonafide tumor suppressor which is capable of suppressing the malignant phenotype of BAP1 null-cells in a transfection assay [(these results are in preparation for submission and are described in detail in this report (see above and appendices)].

3.   We have initiated a comprehension analysis of the mutational status of BAP1 in both primary human breast and lung tumors and in tumor-derived cell lines. Our preliminary results suggest that a low frequency of mutation occurs, however, they often inactivate the UCH enzymatic domain as would be predicted from the results above.

4.   We have begun pilot experiments to determine if BAP1 is involved in the BRCA1 pathway of transcription-coupled DNA repair (TCR). Our exciting preliminary results suggest that BAP1 null-cells have the same TCR defect as BRCA1 null cells. Moreover, transfection of wild-type BAP1 into these cells restores proper TCR.

All of the work described above and the conclusions derived therefrom were performed in accordance with the original statement work (SOW). Each point of the original SOW is addressed below:

STATEMENT OF WORK

Specific Aim 1:   Characterize interaction of BRCA1 and S6.

Task 1: Months 1-4: Establish vectors/reagents/proteins required for association.
Completed, published in references *1, 13*.

Task 2: Months 4-6: Develop in vitro association assy and in vitro kinase assays.
Completed, unpublished because we could not confirm *in vitro* association of proteins.

Task 3: Months 4-6: Determine ability of BRCA1-RF to modulate S6 kinase activity.
Not addressed due to results of TASK 2.

7

Task 4: Months 4-6: Determine if BRCA1 is a substrate of S6 and map regions required.
Not addressed due to results of TASK 2.

Task 5: Months 6-10: Prepare deletions mutations of BRCA1 and S6 kinase to map interaction.
Completed, published in reference 1.

Specific Aim 2:   Characterize the BRCA1 associated protein BAP-1.

Task 6: Months 1-6: Isolate full-length cDNA clones of BAP-1 and genomic clones.
Completed, cDNA clone published in reference 1.
However, genomic clone is not yet published.

Task 7: Months 6-12: Sequence entire cDNA of BAP-1 and determine intron/exon organization of genomic BAP-1.
Completed, in preparation for publication.

Task 8: Months 12-18: Prepare recombinant purified BAP-1 and synthetic peptides to coding region.
Completed, published in reference 13.

Task 9: Months 18-24: Prepare antibodies to BAP-1 both polyclonal and monoclonal and characterize.
Completed, published in references 1, 13 and in preparation.

Task 10: Months 24-30: Isolate in vitro complexes of BRCA1 and BAP-1 via co-immunoprecipitation, and localize BAP-BRCA1 subcellularly. Reconstitute BAP-1/BRCA1 complexes in vitro.
Partially completed. The _in vitro_ association of BAP-1 and BRCA1 are published in reference 1. However, this was from complex mixtures and could, therefore, be indirect binding. We have tried but so far failed to see binding with purified (E-coli expressed) components. BRCA1 and BAP-1 have been co-localized in cells (published in reference 13).

Task 11: Months 30-36: Prepare mutations/deletions of BRCA1 and BAP then map interaction domains.
Completed, published in reference 1.

Task 12: Months 36-42: Determine chromosomal location BAP-1 and promotor structure of BAP-1.

Partially completed: Human BAP-1 chromosomal location was published in reference 1. The promotor structure analysis is ongoing.

Specific Aim 3: Characterize BAP-1/BRCA1 in primary breast cancer specimens and look for mutations in BAP-1.

Task 13: Months 36-42: Using intron-exon structure and PCR-SSCP based studies, look for mutation in BAP-1 in primary specimens.

Partially completed. More than 120 tumors screened so far by PCR-SSCP.

Task 14: Months 42-48: Determine if expression of BAP-1 in cultured breast cancer cells influences BRCA-1 function and also determine if BAP-1 itself is a transforming gene in mammary epithelial cells.

Partially completed (see this write up).

WORK UNDERTAKEN NOT IN ORIGINAL SOW

Because of the clear role of BRCA-1 in DNA repair processes, we have begun analysis of BAP-1 in these pathways. This work is in collaboration with Dr. Tony Leadon from UNC whose group published the seminal work on BRCA1 and its role in DNA repair (reference 9). In collaboration, we have made the exciting initial discovery that BAP1 null cells also have the exact same defect in DNA repair. Furthermore, transfection of wild-type BAP1 corrects the repair defect. These results are currently being prepared for submission to *Science*.

REFERENCES

1.   Jensen, D. E., Proctor, M., Marquis, S. T., Gardner, H. P., Ha, S. I., Chodosh, L. A., Ishov, A. M., Tommerup, N., Vissing, H., Sekido, Y., Minna, J., Borodovsky, A., Schultz, D. C., Wilkinson, K. D., Maul, G. G., Barlev, N., Berger, S. L., Prendergast, G. C., and Rauscher, F. J., 3rd BAP1: a novel ubiquitin hydrolase which binds to the BRCA1 RING finger and enhances BRCA1-mediated cell growth suppression, Oncogene. *16:* 1097-112, 1998.

2.   Wilkinson, K. D. Roles of ubiquitinylation in proteolysis and cellular regulation. [Review] [136 refs], Annual Review of Nutrition. *15:* 161-89, 1995.

3.   Hochstrasser, M. Protein degradation or regulation: Ub the judge. [Review] [15 refs], Cell. *84:* 813-5, 1996.

4.   Zhang, H., Somasundaram, K., Peng, Y., Tian, H., Bi, D., Weber, B. L., and El-Deiry, W. S. BRCA1 physically associates with p53 and stimulates its transcriptional activity, Oncogene. *16:* 1713-21, 1998.

5.   Scheffner, M., Huibregtse, J. M., Vierstra, R. D., and Howley, P. M. The HPV-16 E6 and E6-AP complex functions as a ubiquitin-protein ligase in the ubiquitination of p53, Cell. *75:* 495-505, 1993.

6.   Scully, R., Chen, J., Plug, A., Xiao, Y., Weaver, D., Feunteun, J., Ashley, T., and Livingston, D. M. Association of BRCA1 with Rad51 in mitotic and meiotic cells, Cell. *88:* 265-75, 1997.

7.   Wong, A. K. C., Pero, R., Ormonde, P. A., Tavtigian, S. V., and Bartel, P. L. RAD51 interacts with the evolutionarily conserved BRC motifs in the human breast cancer susceptibility gene brca2, J Biol Chem. *272:* 31941-4, 1997.

8.   Gowen, L. C., Avrutskaya, A. V., Latour, A. M., Koller, B. H., and Leadon, S. A. BRCA1 required for transcription-coupled repair of oxidative DNA damage, Science. *281:* 1009-12, 1998.

9.   Cressman, V. L., Backlund, D. C., Avrutskaya, A. V., Leadon, S. A., Godfrey, V., and Koller, B. H. Growth Retardation, DNA Repair Defects, and Lack of Spermatogenesis in BRCA1-Deficient Mice, Mol Cell Biol. *19:* 7061-7075, 1999.

10.   Shen, Z., Pardington-Purtymun, P. E., Comeaux, J. C., Moyzis, R. K., and Chen, D. J. UBL1, a human ubiquitin-like protein associating with human RAD51/RAD52 proteins, Genomics. *36:* 271-9, 1996.

11.   Shen, Z., Pardington-Purtymun, P. E., Comeaux, J. C., Moyzis, R. K., and Chen, D. J. Associations of UBE2I with RAD52, UBL1, p53, and RAD51 proteins in a yeast two-hybrid system, Genomics. *37:* 183-6, 1996.

12.   Johnson, E. S. and Blobel, G. Ubc9p is the conjugating enzyme for the ubiquitin-like protein Smt3p, J Biol Chem. *272:* 26799-802, 1997.

13.   Maul, G.G., Jensen, D.E., Ishov, A.M., Herlyn, M., and Rauscher, III, F.J. Nuclear Redistribution of BRCA1 During Viral Infection, Cell Growth & Diff. *9:*743-755, 1998.

Appendices

I.   Figure Legends and data figures
II. Published Manuscript

Figure 1. Generation of BAP1 Monoclonal Antibodies and Stable Cell Lines. A, Schematic representation of the human BAP1 protein sequence derived from its cDNA sequence. The general location of the epitopes for the monoclonal antibodies is shown

above the human schematic as is the BRCA1 interaction domain. UCH, ubiquitin carboxyl terminal hydrolase domain. B, Relative reactivity of anti-BAP1 antibodies. In vitro transcribed and translated human BAP1 (BAP1 IVT) was immunoprecipitated using the various antibodies shown and protein G-Sepharose as the precipitating agent. After washing the immunoprecipitated complex, the bound protein was released from the sepharose beads, separated by SDS-PAGE and visualized by fluorography. The polyclonal antibody is derived from rabbit sera (PI=pre-immune sera; Ab=immune sera) and the monoclonal antibodies are supernatants from individual hybridoma lines. C, Detection of endogenous BAP1 by Western analysis in the cell lines listed. One hundred micrograms of nuclear extract (NE) or whole cell extract (WCE) were separated by SDS-PAGE and transferred to a PVDF membrane. The BAP1 protein was then visualized using the 3C11 monoclonal antibody and HRP-conjugated rabbit anti-mouse secondary antibody. D, Western analysis of several sub-clones of the NCI-H226 cell line showing the different expression levels of BAP1 or BAP1(C91S). Whole cell extracts from logarithmically growing cells were separated by SDS-PAGE and transferred to a PVDF membrane. The BAP1 protein was visualized using the 3C11 monoclonal antibody and HRP-conjugated rabbit anti-mouse secondary antibody.

Figure 2. Cell lines expressing wild-type BAP1 show decreased growth rates in response to reduced mitogenic factors. Sub-clones of the NCI-H226 cell line expressing none, wild-type, or mutant BAP1 were grown in RPMI1640 medium containing 2% FCS. Cell growth rates were determined by the MTT assay (see Materials and Methods). Error bars represent Std. Error of the mean (SEM). The number of replicates is shown in parentheses above the bar. There was no difference in growth rate between the parental line (NCI-H226) and those containing vector alone.

Figure 3. Cell lines expressing wild-type BAP1 show a change in cell morphology, but no change in anchorage-independent growth. Cells were grown directly on plastic tissue culture dishes or on 0.6% agarose (in plastic tissue culture dishes) and photographed at 2 days (plastic) or 21 days (soft agar). Shown are representative examples of each type of cell line. 4X magnification.

Figure 4. Tumors from SCID mice maintain expression of BAP1(C91S), but not wild-type BAP1. A, Whole cell extracts made from tumors of each of the mice in experiment #1 (Table #1) were analyzed for BAP1 expression by Western analysis using the 3C11 monoclonal antibody and HRP-conjugated rabbit anti-mouse secondary antibody.. B, Whole cell extracts were made from tumors of 5 of the Vector mice and from each of the BAP1(C19S) mice of experiment #2 (Table #1). These extracts were analyzed for BAP1(C91S) expression by Western analysis using the 3C11 monoclonal antibody and HRP-conjugated rabbit anti-mouse secondary antibody. An alpha-tubulin monoclonal antibody was used as a control for equivalent protein loading in both analyses.
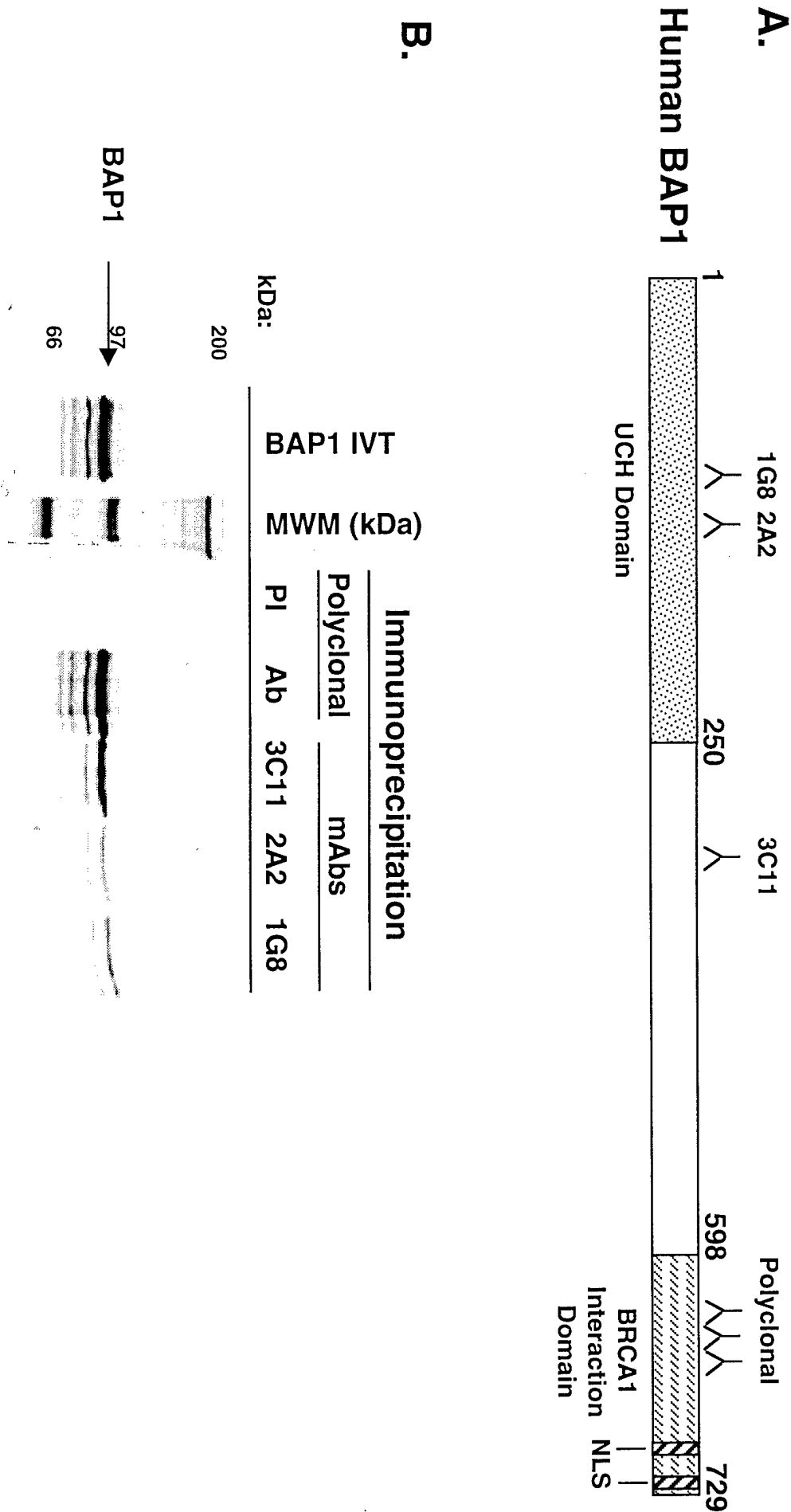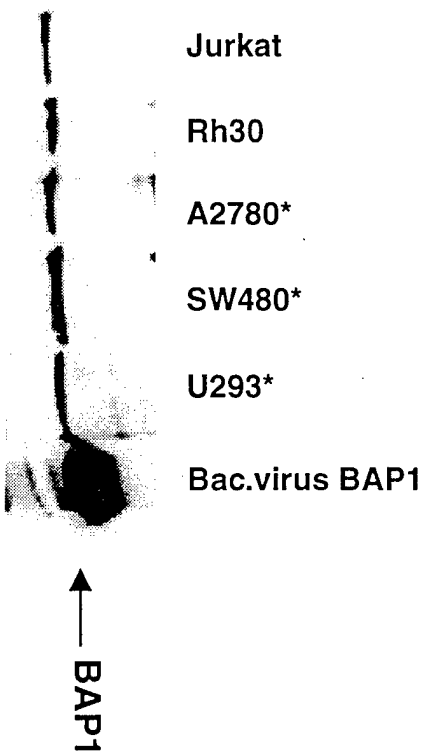
Figure 1

Figure 1

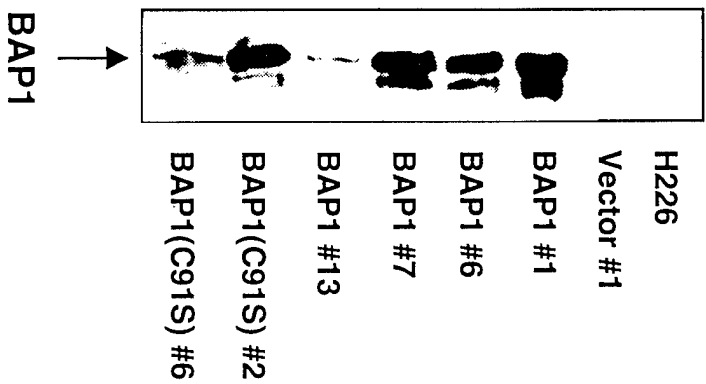## C.   Cell line western

* Nuclear Extracts

Jurkat

Rh30

A2780*

SW480*

U293*

Bac.virus BAP1

← BAP1

D.

BAP1 →

BAP1(C91S) #6

BAP1(C91S) #2

BAP1 #13

BAP1 #7

BAP1 #6

BAP1 #1

Vector #1

H226

Figure 2

Figure 3

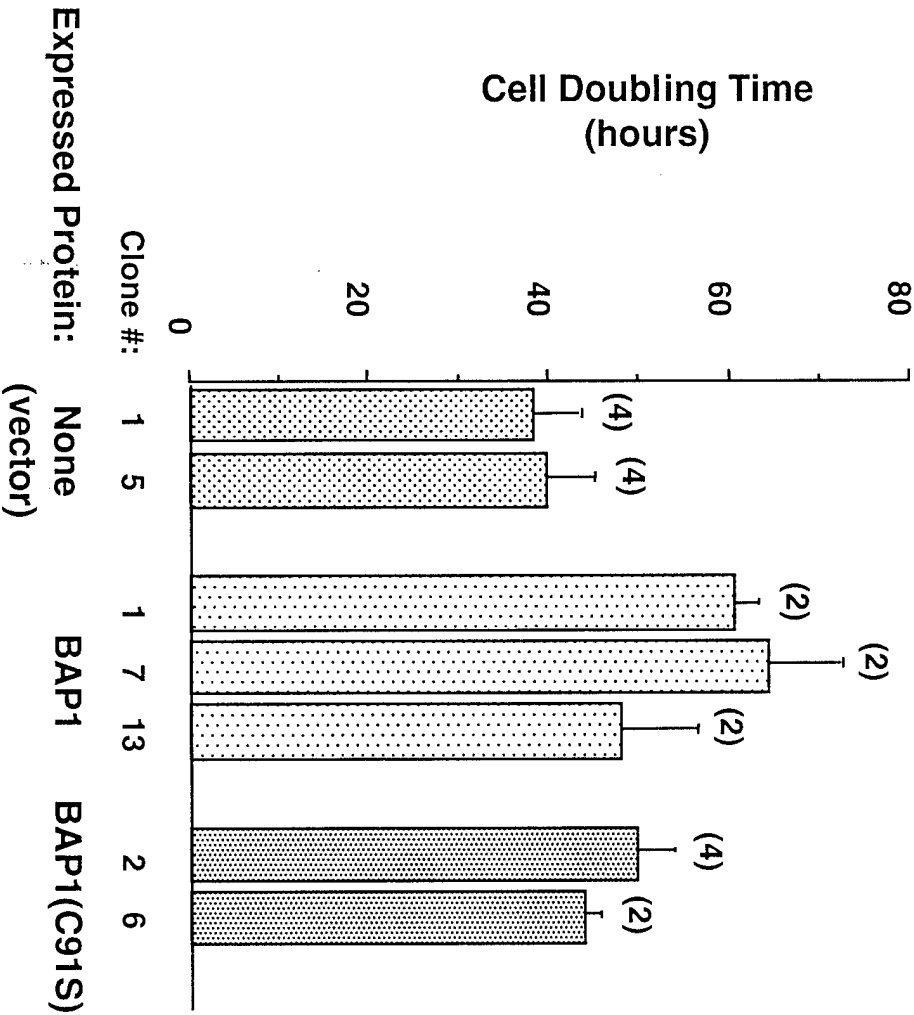Soft Agar

Plastic
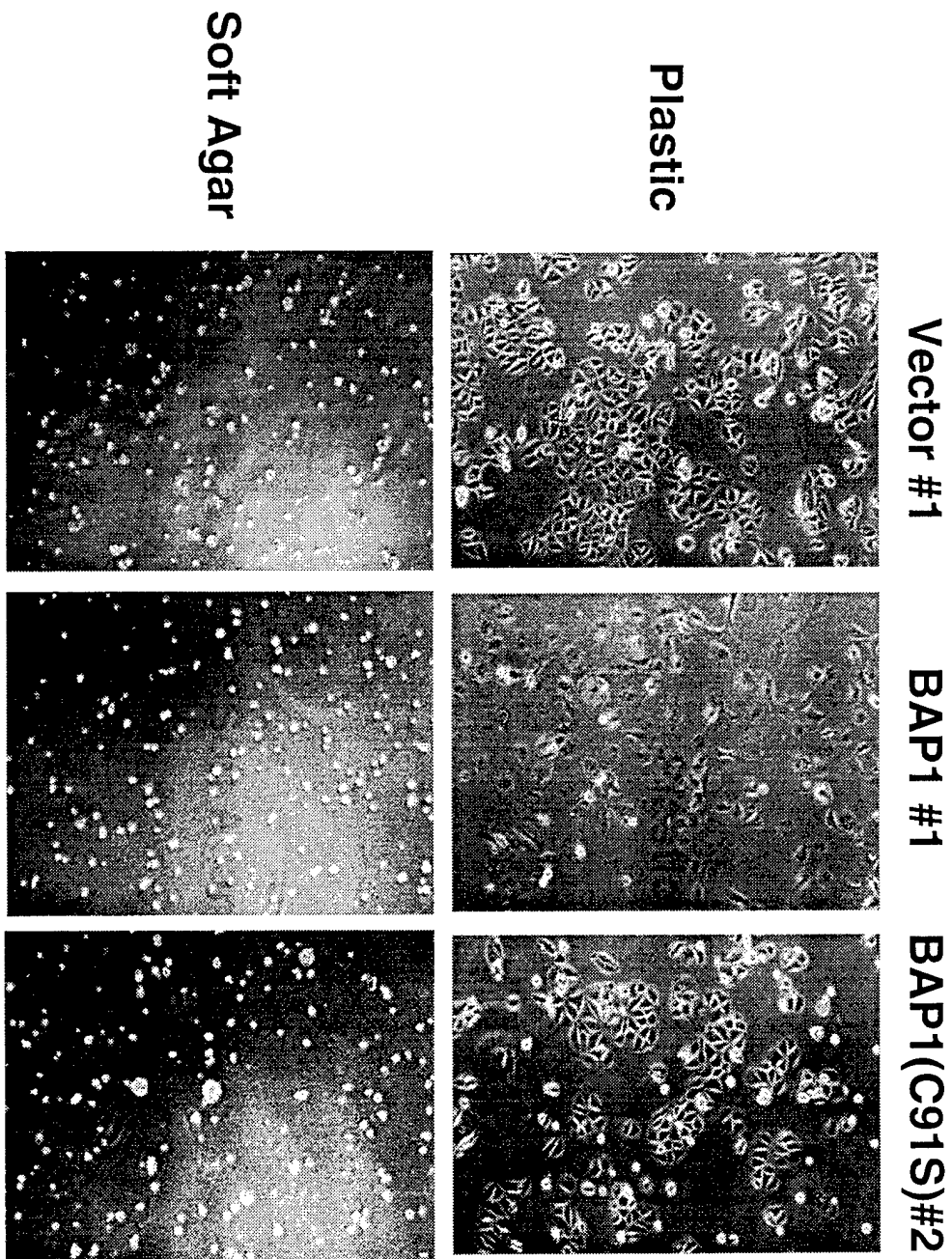
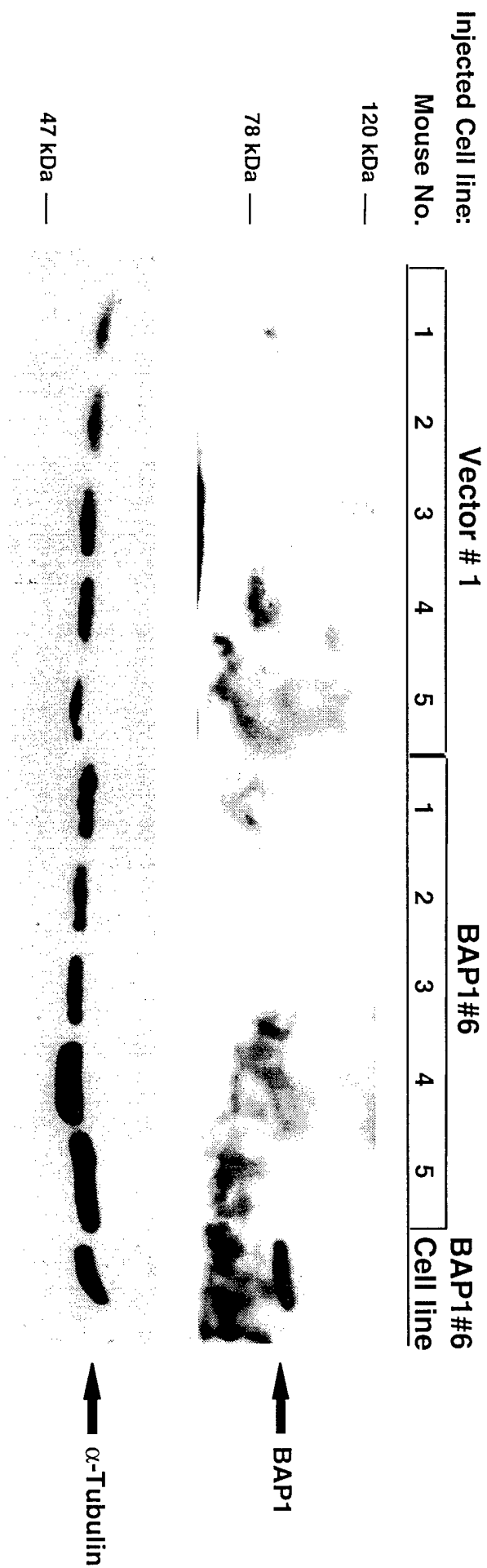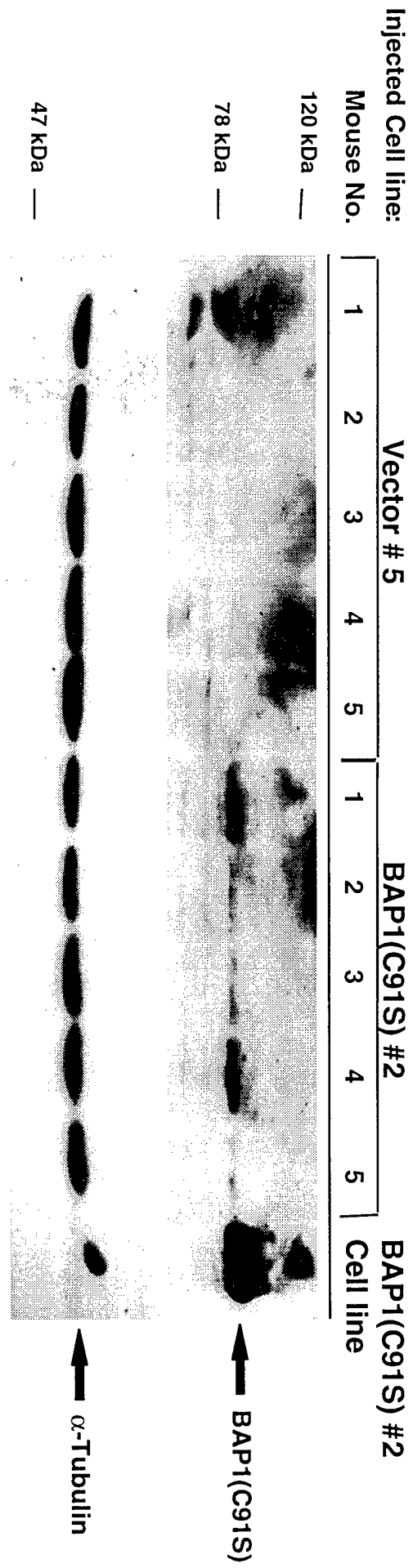Vector #1   BAP1 #1   BAP1(C91S)#2

Figure 4A

Figure 4B

Table 1.   Average Tumor Size in SCID mice given s.c. injections of the NCI-H226 cell line expressing none (vector), wild-type, or mutant BAP1[a]

	Expt. #1[b]	Expt. #2[c]
Vector	1.27 ± 0.65 cm³ (5)	0.84 ± 0.42 cm³ (8)
BAP1	0.11 ± 0.08 cm³ (5) [d]	No Tumors (5) [d]
BAP1(C91S)	(N/D)	0.78 ± 0.29 cm³ (5)

[a]Values are expressed as mean ± Std.Dev.
[b]Mice were injected with 5X10⁶ cells and the tumors were harvested 42 days later.
[c]Mice were injected with 5X10⁶ cells and the tumors were harvested 30 days later.
[d]$P < 0.01$ versus vector (t-test).

Nuclear Redistribution of BRCA1 during Viral Infection[1]

Gerd G. Maul,[2] David E. Jensen, Alexander M. Ishov, Meenhard Herlyn, and Frank J. Rauscher, III

The Wistar Institute, Philadelphia, Pennsylvania 19104

Abstract

The functions and the intracellular localization of the breast/ovarian susceptibility gene product, BRCA1, has been controversial. To arrive at a clear understanding of its localization and relative position to other nuclear structures, a new monoclonal antibody was produced and characterized by immunohistochemical techniques with other BRCA1 antibodies. Each of the antibodies specifically detected BRCA1 as localized to specific nuclear domains and did so in a variety of cells and in a cell cycle-dependent manner. However, all antibodies also cross-reacted with the centrosomal domain, suggesting that BRCA1 is also localized to this important mitotic component. We found that the BRCA1-containing nuclear domains are different than any of the well-defined nuclear domains. However, a cell cycle-related partial overlap was found for HP1α, a chromo-domain-containing protein involved in heterochromatin maintenance. Cellular stimuli, such as heat shock and herpes virus infection, dispersed BRCA1 from its domains. In contrast, infection with adenovirus 5 recruited BRCA1 to regions of viral transcription and replication. These disparate distributions of BRCA1 may provide clues to its function.

Introduction

The identification of the breast cancer susceptibility gene *BRCA1* (1) has triggered an intensive search for its function. Much of this search has focused on the identification of interacting proteins and has yielded components of the nuclear import pathway (2) and a novel RING finger-containing protein BARD1 (3, 4). Recently, we identified the BRCA1-associated protein BAP1 (5), which is a nuclear localized ubiquitin hydrolase, suggesting that BRCA1 functions may be either mediated or regulated through ubiquitin-related

modifications. BRCA1 also seems to be associated with the DNA recombination/repair protein RAD51 in meiotic cells (6), suggesting involvement of BRCA1 in the fidelity of DNA replication. Biological clues to the function(s) of BRCA1 have come through over- or underexpression studies. A reduction in BRCA1 availability by antisense expression yielded transformed fibroblasts and accelerated growth of breast cancer cell lines (7, 8), whereas overexpression of wild-type BRCA1 inhibited colony formation and tumor growth *in vivo* (9). These observations are consistent with the genetic evidence that BRCA1 functions as a tumor suppressor (5, 9).

The *BRCA1* gene encodes an 1863 amino acid protein of M_r ~220,000, which is predominately found within the nucleus (4, 10), although some investigators have observed cytoplasmic localization (11, 12). The BRCA1 protein contains two highly conserved regions, one at the NH_2 terminus and the other at the COOH terminus. The COOH terminus contains an acidic region and two copies of a novel motif, designated the BRCT domain. The BRCT domain is present in a variety of putative cell cycle-related proteins, including RAD9 and 53BP1 (13), as well as the BRCA1-associated protein BARD1 (3). The BRCA1 COOH-terminal domain is capable of activating transcription as a Gal4 DNA-binding domain fusion (14), suggesting a role for BRCA1 in transcriptional regulation. The cofractionation of BRCA1 with the RNA pol II holoenzyme (15) supports this hypothesis. However, not all of the cellular BRCA1 cofractionates with pol II, suggesting multiple functions for BRCA1.

The NH_2-terminal region is a 100-amino acid sequence encoding a RING finger domain, which is predicted to bind zinc (16, 17). This motif is defined by a spatially conserved set of cysteine-histidine residues of the form C3HC4 (reviewed in Refs. 18 and 19). The RING motif occurs in >80 proteins, including the products of proto-oncogenes and putative transcription factors (19), and most likely functions as a protein-protein interface. Evidence for this hypothesis has come from the study of the proto-oncogene *PML* (16), the transcriptional corepressor KAP-1 (20), and a ubiquitin hydrolase, BAP1 (5).

The abundance and intracellular location of BRCA1 varies with the cell cycle. BRCA1 protein levels are low in G_1 and reach a maximum during S phase, results that are consistent with BRCA1 RNA expression patterns (21–24). Interestingly, the location of BRCA1 within the nucleus seems to vary with the cell cycle. BRCA1 is detected as diffuse immunofluorescent staining throughout the nucleus during G_1 but then localizes to discrete nuclear domains during S phase (4, 10). The functional effects of these cellular and biochemical changes remain unknown.

The nucleus is a highly organized structure, not only in the positioning of chromosomes in specific territories, but also by the distribution of extrachromosomal domains, *e.g.*, the interchromatinic granules recognizable by the location of the spliceosome assembly factor SC35 (25, 26). In addition,

coiled bodies were found to be associated with specific genes and snRNA and associated proteins (27–30). PIKA is a nuclear domain that shows cell cycle-associated changes in the aggregation of HP-1 (31). Other specifically circumscribed nuclear domains (ND10) have been described to contain the proto-oncogene product PML as well as Int-6, which, if interrupted in the mouse by a retrovirus, results in mammary tumors (32, 33). Although the biochemical functions of these domains are not known, various nuclear processes, such as RNA processing (SC35 domain) and initiation of DNA virus replication and transcription (34, 35), occur at these domains. Because BRCA1 is also localized to discrete nuclear domains, potential functions of BRCA1 may be suggested, or excluded, by interaction or colocalization with any of the known nuclear domains. The relative position of BRCA1 in the nucleus may therefore be informative.

Recent findings on nuclear structure and distribution of specific proteins after viral infection showed that some of these proteins are modified at specific stages of viral infection. Most instructive are those proteins that appear at very early times of the viral reproductive cycle before nuclear damage becomes apparent and which can be traced to the activity of a specific immediate-early protein. The IE1 gene product of HSV[3] type 1 disperses the ND10-associated proteins (36–38), and the E4orf3 gene product of Ad5 repositions the same proteins into short tracks (39–41). We therefore used these viruses to determine whether they have any effect on BRCA1 distribution.

The ability to establish colocalization of two proteins by microscopic examination suggested that this methodology could be used as a means to search for other correlations of either the nuclear sites with known functions or for conditions that change the distribution of BRCA1. We therefore developed a MAb that reliably localized BRCA1 relative to different nuclear domains. The results of these experiments clearly show that BRCA1 is a protein with dramatic nuclear repositioning during the cell cycle and upon experimental manipulations of the cell such as stress and viral infection. These changes suggest that Ad5 transcription and replication can provide the experimental system to help elucidate BRCA1 functions.

Results

Characterization of MAb BR64. To determine possible functions for BRCA1, we investigated its subcellular localization and its potential colocalization with a variety of known nuclear proteins of differing function. Investigation of the subcellular localization of BRCA1 required a well-characterized, highly specific antibody. Toward this end, we developed a MAb specific for BRCA1, using the first 100 amino acids of the BRCA1 protein as the antigen (Fig. 1A). This region was expressed in *Escherichia coli* as a histidine fusion protein, purified under denaturing conditions and renatured by dialysis (see "Materials and Methods" and Ref. 20). This

purified protein was used as the immunizing agent in mice, and MAbs were produced using standard technology.
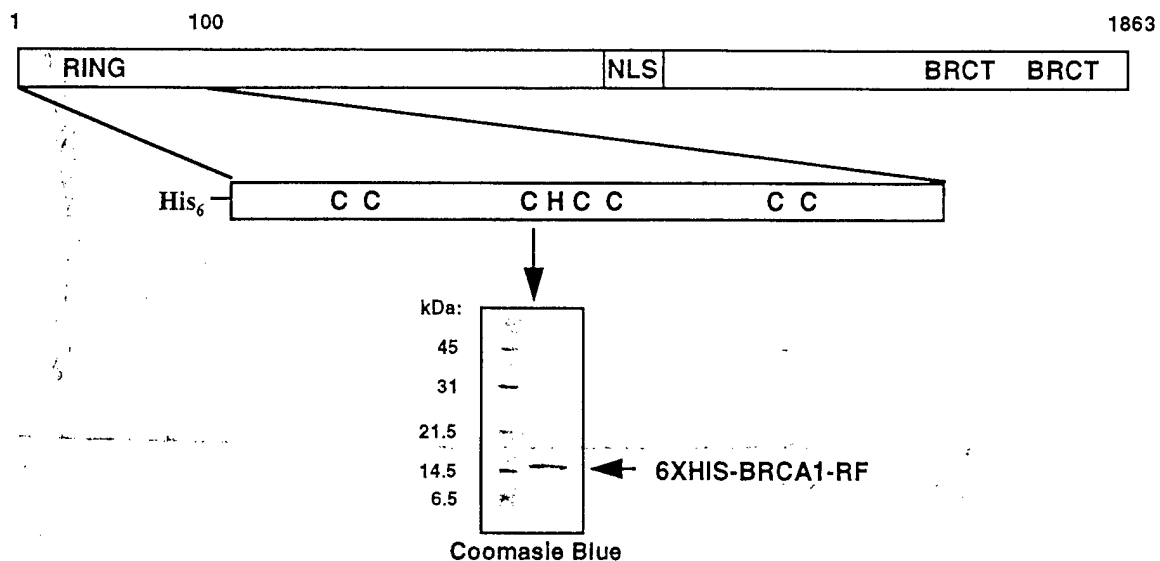
Because the immunizing antigen contains the RING finger domain of BRCA1 and because many proteins contain RING domains, we determined the specificity of our MAb, termed BR64, for the BRCA1 RING domain *versus* the RING domains of two other, unrelated proteins; the transcriptional corepressor KAP-1 and the immediate-early protein ICP0, from HSV type I. Through immunoprecipitation analyses with the BR64 antibody, we found that it detected the BRCA1 RING domain in both the full-length protein and the smaller BRCA1-Δ11 protein (an alternatively spliced version of BRCA1; Ref. 42) but not either of the other RING domains (Fig. 2A), suggesting that the antibody identifies a sequence-specific region of BRCA1 rather than a structural component of the RING finger, which may be in common with other RING domains.

Mutations occur throughout BRCA1, and most are truncations or nonsense mutations (43). Given that the epitope of this antibody is at the NH_2 terminus of the protein, it should detect all except the shortest BRCA1 mutant proteins. Therefore, we characterized whether BR64 could identify BRCA1 protein that contained any one of several mutations identified previously in breast cancer kindreds, focusing on mutations found in the RING domain (Fig. 1B). We used proteins that contained the LexA DNA binding domain fused to: (a) the first 100 amino acids of BRCA1 (BRCA1-RF); (b) this same region but containing a missense mutation in a metal-coordinating cysteine residue [BRCA1-RF(C61G) and BRCA1-RF(C64G)]; or (c) a truncated BRCA1-RF containing the appropriate number of amino acids as dictated by the mutation (delAG185, 29 amino acids; del31, 31 amino acids). The RING domain of the T-cell transcription factor RPT-1 (44), the most closely related RING finger sequence, was also included. Again, immunoprecipitation analysis was used to identify proteins bound by the BR64 antibody (Fig. 2B). The BR64 antibody identified only those proteins that contained the full RING domain region, regardless of the presence or absence of missense mutations (Fig. 2B). Again, these results suggest that the BR64 antibody identifies a sequence-specific region of BRCA1, rather than a structural component of the RING finger, because the missense mutations are predicted to abolish the coordination of one of the zinc atoms leading to the disruption of the complex RING structure (16). The fact that the RING domain of the RPT-1 protein was not identified by BR64 further suggests that the antibody identifies a sequence-specific domain within BRCA1. The proteins fused to the LexA DNA-binding domain always appeared as doublet bands on SDS-PAGE. This was true for the LexA DNA-binding domain alone as well (data not shown) and is presumably due to an alternate, in-frame, translation start site within the LexA cDNA.

We determined the subregion within the NH_2 terminal 100 amino acids of BRCA1 that the BR64 MAb detects. LexA-BRCA1-RF fusion proteins, containing successive 10-amino acid deletions from the COOH terminus of the 100-amino acid BRCA1 RING finger protein, were immunoprecipitated with the BR64 MAb (Fig. 1B and Fig. 2C). The BR64 MAb detected the full-length RING finger domain [BRCA1 (1–100)]

---

[3] The abbreviations used are: HSV, herpes simplex virus; Ad, adenovirus; MAb, monoclonal antibody; FBS, fetal bovine serum; His, histidine; h.p.i., hours post infection.

A.

1   100   1863

| RING | | NLS | | BRCT BRCT |

His₆ — | C C   C H C C   C C |

kDa:
45
31
21.5
14.5 ◄— **6XHIS-BRCA1-RF**
6.5

Coomasie Blue

**MAb BR64
Interaction**

B.

BRCA1-RF   LexA   C C C H C C   C C   (1–100)   ++

BRCA1(1-90)   LexA   C C C H C C   C C   (1–90)   +

BRCA1(1-80)   LexA   C C C H C C   C C   (1–80)   —

BRCA1(1-70)   LexA   C C C H C C   C C   (1–70)   —

BRCA1(C64G)-RF   LexA   C C C H C C   C G   (1–100)   ++

BRCA1(C61G)-RF   LexA   C C C H C C   G C   (1–100)   ++

BRCA1-delAG185   LexA   (22–39)   —

BRCA1-del31   LexA   C C   (31 35)   —

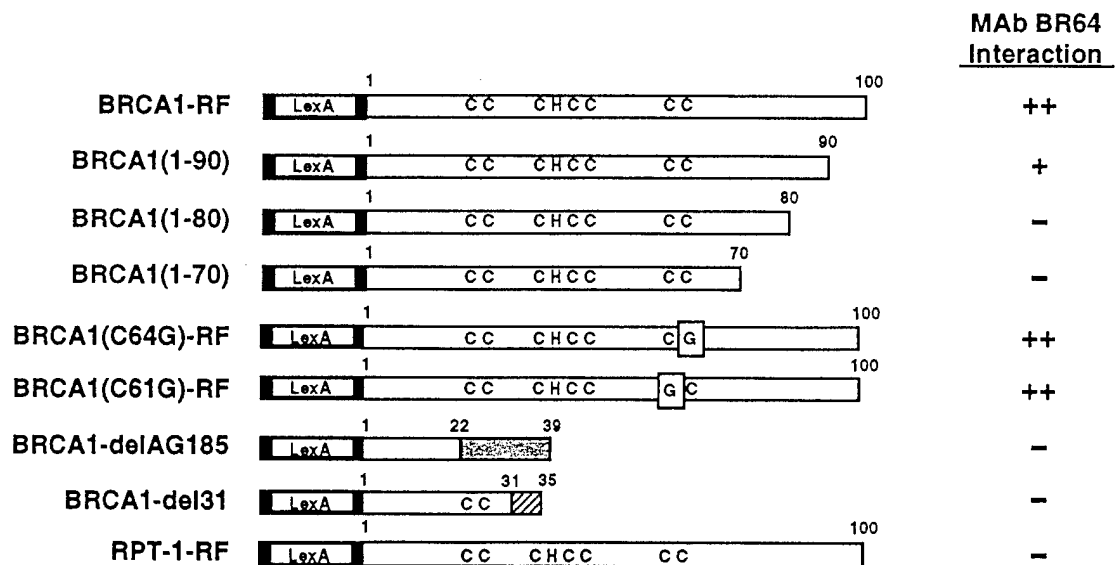**RPT-1-RF**   LexA   C C C H C C   C C   (1–100)   —

Fig. 1. A, diagrammatic representation of the BRCA1 protein and the RING finger domain used to generate the 6XHis-BRCA1-RF fusion protein. The identified fusion protein was produced in bacteria, purified by nickel-NTA chromotography (Qiagen, Inc.), and analyzed by SDS-PAGE for purity. Shown is a photograph of the Coomassie blue-stained gel. In *B,* the NH₂-terminal 100 amino acids of human BRCA1 (including the RING finger domain) or the indicated amino acids of the various BRCA1-RF mutants, deletions, and controls were fused to the LexA DNA-binding domain. These constructs were then used to produce the fusion protein by coupled *in vitro* transcription and translation. These proteins were used without further purification in immunoprecipitation analyses with the BR64 MAb. A summary of the results shown in Fig. 2 is shown to the *right* of the diagrams.

and the RING domain truncated by 10 amino acids [BRCA1 (1–90)]. The 20- and 30-amino acid deletions, BRCA1 (1–80) and BRCA1 (1–70), were not detected by BR64, clearly indicating that amino acids 80–100 contain the region identified by BR64. Indeed, preincubation of the BR64 antibody with a 14-amino acid peptide (amino acids 81–94; H-KKK-QLVEELLKIICAFQ-KK-OH) inhibited the detection of BRCA1 by immunofluorescence analysis (data not shown). These

analyses suggest that the BR64 antibody detects an epitope COOH-terminal to the C3HC4 motif, which defines the RING domain proper.

The ability of BR64 to detect authentic, endogenous BRCA1 protein was determined through three methodologies; immunoprecipitation; immunoprecipitation followed by Western blot analysis; and direct Western blot analysis of nuclear extract. That BR64 detected BRCA1 was determined
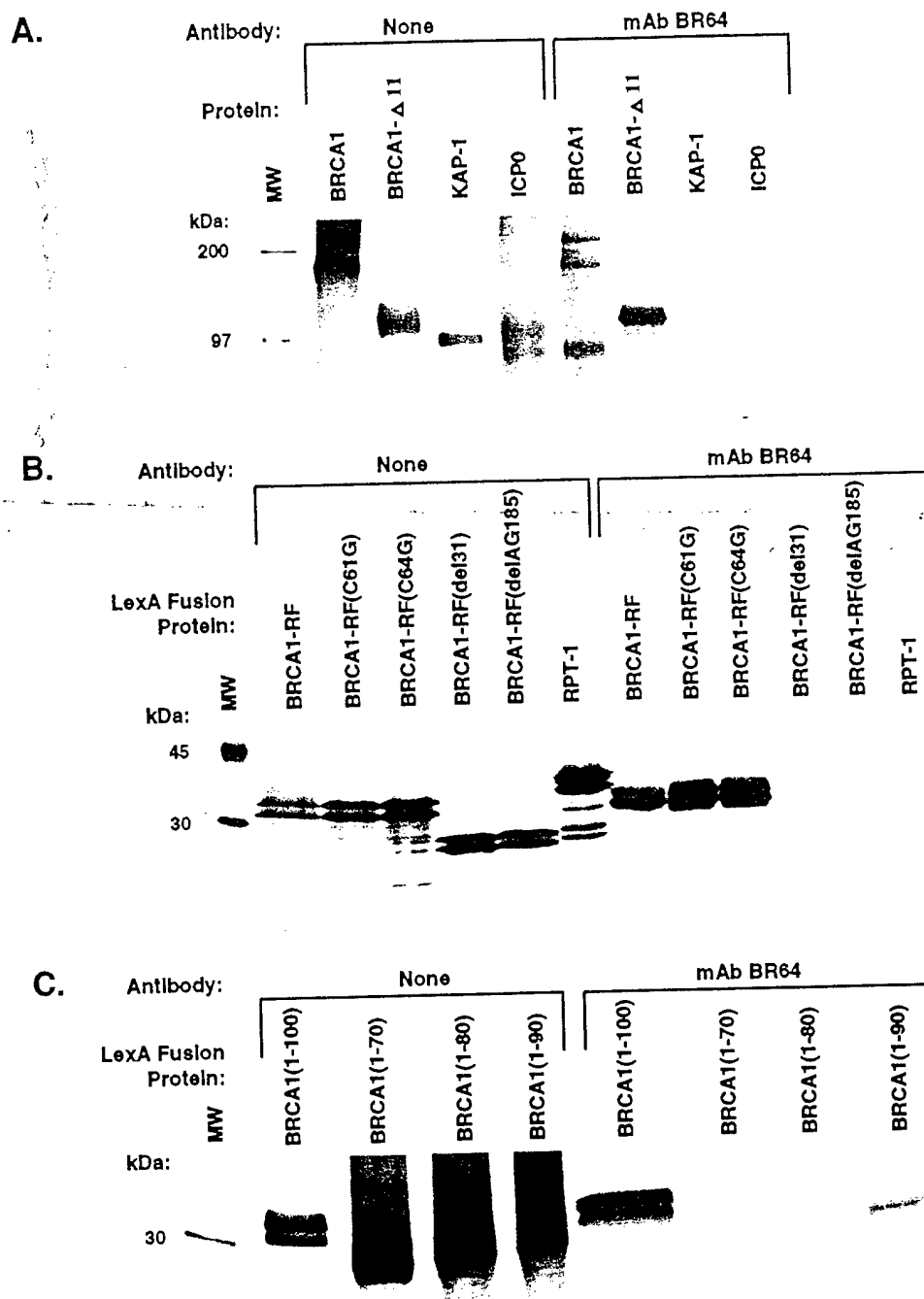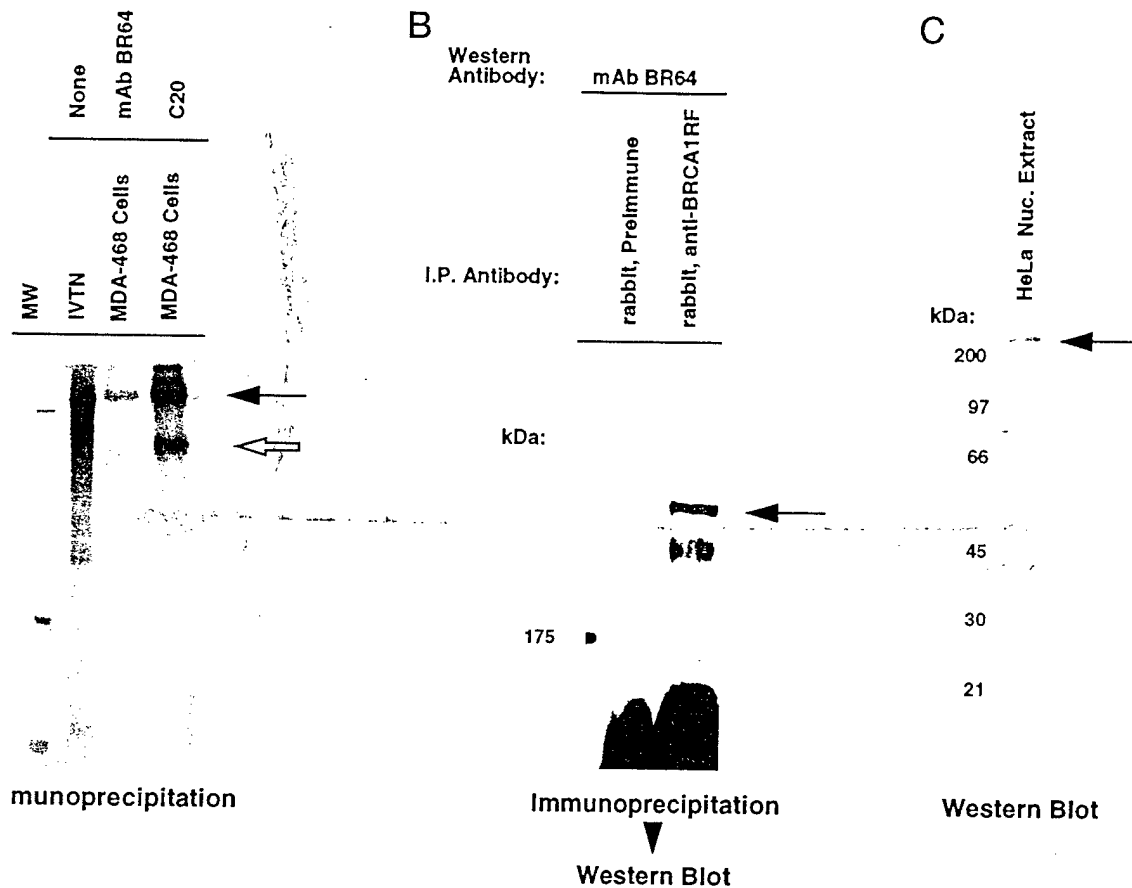
A.

B.

C.

Fig. 2. In *A*, the BR64 MAb detects only the BRCA1 RING finger domain. The indicated RING finger-containing proteins were transcribed and translated *in vitro* in the presence of [^{35}S]methionine. They were then immunoprecipitated with the BR64 MAb, and the bound proteins were separated by SDS-PAGE. Proteins were then detected by fluorography. Faster-migrating proteins detected by the BR64 MAb in the BRCA1 lane are most likely proteolytic fragments of BRCA1. The appearance and intensity of these proteins varied with each *in vitro* transcription-translation reaction. In *B*, BRCA1 RING finger domains containing missense mutations can be detected by BR64. Mutations found in breast cancer kindreds were introduced into LexA-BRCA1-RF fusion proteins. These proteins were transcribed and translated *in vitro* in the presence of [^{35}S]methionine, followed by immunoprecipitation with the BR64 MAb. Bound proteins were separated by SDS-PAGE and detected by fluorography. LexA-RPT-1 is a fusion protein containing the RING finger domain from the RPT-1 protein. In *C*, amino acids 80–100 of the BRCA1 protein contain the epitope for the BR64 MAb. Truncated LexA-BRCA1-RF fusion proteins were transcribed and translated *in vitro* in the presence of [^{35}S]methionine and then immunoprecipitated with the BR64 MAb. Bound proteins were detected by fluorography after separation by SDS-PAGE. Proteins fused to the LexA DNA-binding domain always appear as doublet bands on SDS-PAGE. This is true for the LexA DNA-binding domain alone as well (data not shown) and is presumably due to an alternate, in-frame, translation start site within the LexA cDNA.

by a comparison of the products immunoprecipitated from whole-cell extracts of $^{32}PO_4$-labeled MDA-468 breast cancer cells by the BR64 MAb and the commercially available C20 polyclonal antibody (Fig. 3*A*). Both antibodies identify a M_r 220,000 phosphoprotein, suggesting that the protein detected by BR64 is BRCA1. Furthermore, BRCA1 is the only phosphoprotein detected by BR64, whereas the C20 antibody detects three other phosphoproteins of M_r 190,000, M_r 97,000, and M_r 70,000.

A second piece of evidence that the endogenous protein detected by BR64 is BRCA1 was obtained via immunopre-

cipitation-Western analysis (Fig. 3*B*). Whole-cell extracts prepared from HBL100 breast cancer cells were immunoprecipitated with either (rabbit) preimmune serum or anti-BRCA1 immune serum. The immunoprecipitated proteins were then analyzed by Western blot. The BR64 MAb detected a protein of M_r 220,000 previously immunoprecipitated by a specific anti-BRCA1 antibody. However, BR64 also detected a second, faster migrating protein. To address the possibility that BR64 interacted with another protein of large molecular weight, direct Western analysis of nuclear extract from HeLa cells was performed (Fig. 3*C*). The BR64

B

C

Western
Antibody: mAb BR64

I.P. Antibody:

rabbit, Preimmune

rabbit, anti-BRCA1RF

None

mAb BR64

C20

MW

IVTN

MDA-468 Cells

MDA-468 Cells

HeLa Nuc. Extract

kDa:

200

97

66

kDa:

175

45

30

21

munoprecipitation

Immunoprecipitation
▼
Western Blot

Western Blot

10 μm **D**

10 μm **H**

10 μm **K**

ects endogenous BRCA1 protein. In *A*, whole-cell extracts from $^{32}PO_4$-labeled MDA-468 breast cancer cells (5–7 × 10^6 cells) were
·d with the BR64 MAb or the C-20 polyclonal antibody. A BRCA1 cDNA was transcribed and translated *in vitro* in the presence of
produce protein for size comparison purposes. Proteins were separated by SDS-PAGE and detected by fluorography. In *B*, whole-cell
breast cancer cell line HBL-100 (1–2 × 10^6 cells) were immunoprecipitated with preimmune sera or with anti-BRCA1-RF polyclonal
munoprecipitated proteins were separated by SDS-PAGE and transferred to a polyvinylidene difluoride membrane. The membrane was
:h the BR64 MAb and detected with HRP-conjugated goat anti-mouse IgG. In *C*, nuclear extract from HeLa cells was separated by
ansferred to a polyvinylidene difluoride membrane. The membrane was immunoblotted with the BR64 MAb and detected with alkaline
ıgated goat anti-mouse IgG.

ınly a single protein of M_r 220,000, the size of
together, these results show that BR64 iden-
RCA1 protein, can identify native and dena-
·otein, and has an epitope defined by amino
·he faster migrating protein of Fig. 3*B* remains
ɔ is not seen in the immunoprecipitation-
alysis when other anti-BRCA1 antibodies are
ɔhown).

of Different BRCA1 Antibodies. Initial re-
A1 was localized to the cell membrane and
·atus and was perhaps secreted (12) have
·icant controversy. It was therefore essential
the earlier reports could be confirmed with
When the BR64 MAb was tested by immu-
l methods, it reacted nearly exclusively with
nucleus. However, not all cells showed the
n as reported previously by others (10). Nu-
s displayed a sandy fluorescence where as
ddition, distinctly higher aggregations of the
. There was a faint background staining over

the cytoplasm, and often two dots were recognized at the
position of the centrosome (Fig. 4*A, arrow*). Another anti-
BRCA1 MAb, M13 (see "Materials and Methods"), recog-
nized the same nuclear patterns (HEp-2 cells) with slightly
elevated cytoplasmic staining. In a few cells, particularly
mitotic cells, M13 detected numerous cytoplasmic dots over
a strong cytoplasmic background (Fig. 4*B*). A third anti-
BRCA1 MAb, 17F8 (see "Materials and Methods"), labeled a
large number of cytoplasmic dots in all cells. Nuclear staining
by this MAb was difficult to distinguish from the cytoplasmic
staining. but it appears similar to that of the other two MAbs.
In addition, each cell stained by 17F8 contained an area of
strong staining that localized to the centromeric region and
appeared at times to overlap with the nucleus when imaged
in the same optical section (Fig. 4*C, arrows*; optical sections
are ~0.7-μm thick). A rabbit antibody (C20; Santa Cruz),
raised against the COOH-terminal 20 amino acids of BRCA1,
labeled the same nuclear components as all three MAbs (Fig.
4*D*) but also stained the Flemming body (data not shown)
and, in a few cells, a limited number of cytoplasmic granules.
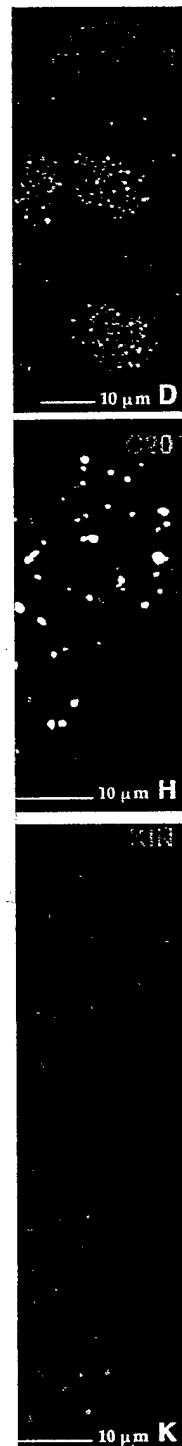
icroscopy. The color
ɔ cytoplasmic double
-labeled HEp-2 cells.
t fibrillar cytoplasmic
ɔ polyclonal antibody
to show in the upper
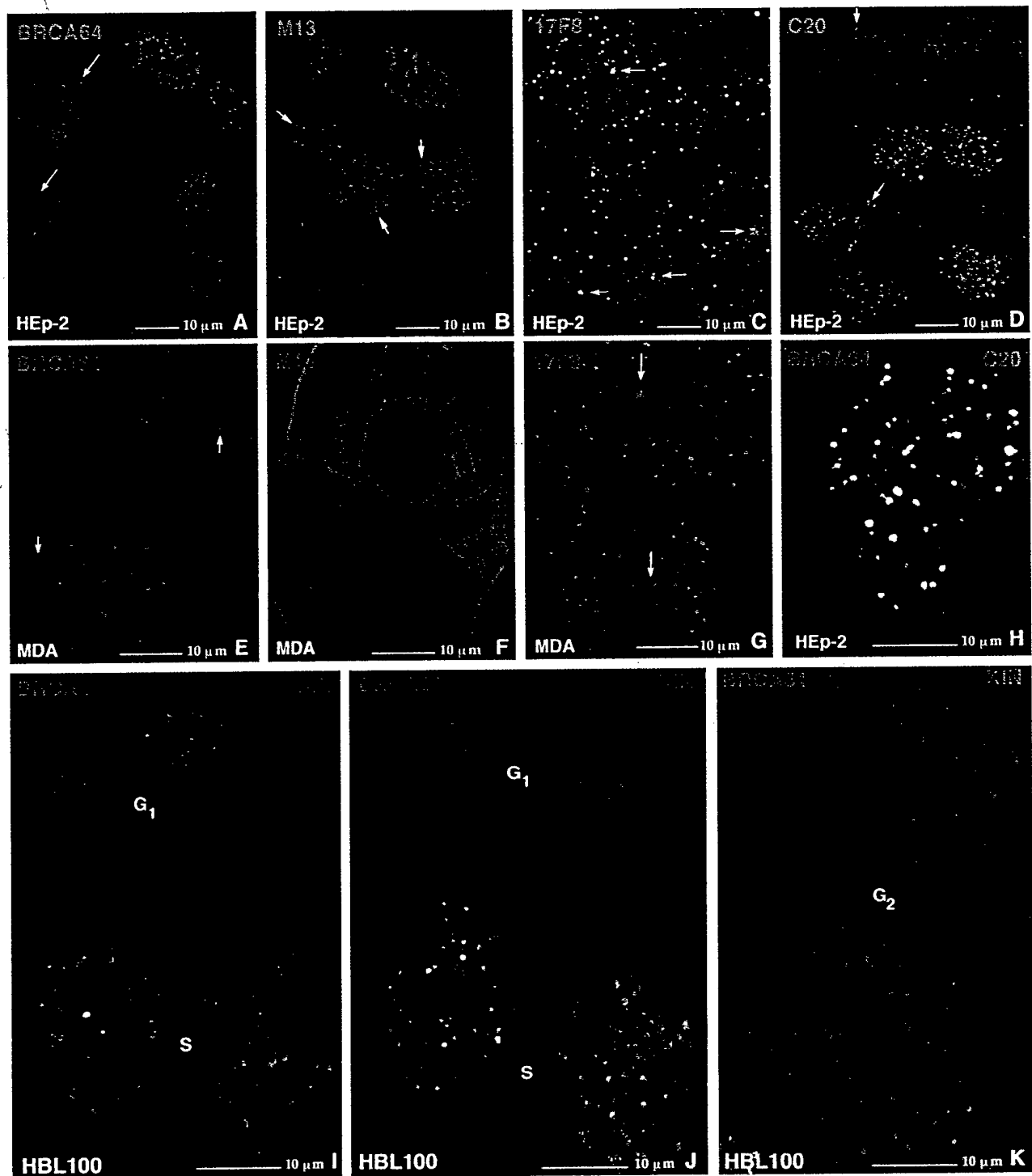ıll at a later time after
ıith centromeres that

Fig. 4. Characterization of BRCA1 distribution in different cells and relative to different nuclear domains by immunofluorescence microscopy. The color is given for each of the different antigens in the *upper corners* of each individual image. *A,* MAb BR64-labeled HEp-2; *arrows* point to cytoplasmic double dots representing the centrosome. *B,* MAb M13-labeled HEp-2 cells. *C,* MAb 17F8-labeled HEp-2 cells. *D,* polyclonal antibody C-20-labeled HEp-2 cells. *E,* MAb BR64-labeled MDA-MB-468 cells; *arrows* point to the centrosome. *F,* MAb M13-labeled MDA-MB-468 cells showing dominant fibrillar cytoplasmic staining. *G,* MAb 17F8-labeled MDA-MB-468 cells showing strong staining of cytoplasmic granules. *H,* double labeled HEp-2 cells using polyclonal antibody C-20 and BR64 showing complete overlap. *I,* double labeled HBL-100 cells using MAb BR64 and human anti-centromere antibodies to show in the upper half daughter cells in early G_1 phase and larger daughter cells with aggregated centromeres. *J,* same as *I* but showing a G_1-phase cell at a later time after mitosis and two larger cells with aggregated centromeres suggestive of S-phase cells. *K,* same staining as *I* having two large cells with centromeres that are often present as doublets suggestive of G_2-phase cells. All optical sections are ~0.7 μm thick

That the new MAb BR64 recognizes the same nuclear structures as C20 is shown by double labeling (Fig. 4*H*). The BRCA1 distribution detected in HEp-2 cells by these antibodies was also found in the diploid human fibroblast cell line WI38 and the breast cancer cell line HBL100 (data not shown). The different antibodies, therefore, recognize the same structural components in the nucleus but appear to have individual, minor, cross-reactivities. We conclude that, in general, the sandy nuclear staining of some cells and the specific nuclear domain dot-like staining of other cells is similar for all of the antibodies and is therefore considered specific for the location of BRCA1.

Quite different images were prevalent when testing these four antibodies on the breast cancer cell line MDA-MB-468. Only a very small number of these breast cancer cells had any particulate, nuclear BRCA1 staining, although the images presented were selected to contain one nucleus with such staining to show that this distribution can exist in this cell type. BR64, of the four antibodies tested, revealed the same image as expected from the Hep-2 cells (Fig. 4*E*, *arrows* point to centrosomes). MAb M13 labeled a particular type of cytoplasmic filament (Fig. 4*F*). In mitotic cells, these fibers disappeared and resulted in cytoplasmic dots. MAb 17F8 recognized a large cytoplasmic component similar to those in HEp-2 cells and stained the centrosomes (Fig. 4*G*, *arrows*). None of the antibodies reliably showed the nuclear BRCA1 staining anticipated from the other cell types. The absence of BRCA1 staining may be used as an indication of a lower concentration of BRCA1 in these nuclei and demonstrates the diversity of cross-reactivities of these antibodies.

Cell Cycle-related Nuclear Distribution of BRCA1. We asked whether the appearance of disparate BRCA1 distributions might be due to changes in the cell cycle as reported previously (4, 10, 45). This was tested by comparing the BRCA1 distribution pattern with cell size and the distribution of centromeres. Centromeres are present in singles very early during the cell cycle, aggregate in late G_1 and S phases, and can be found in doublets after the late S-phase replication of satellite DNA (46). Very early G_1-phase cells remain connected and show the Flemming body, and as shown in Fig. 4*I*, these daughter cells have no discreet BRCA1 domains. In contrast, the larger daughter cells have distinct BRCA1 accumulation and contain aggregated centromeres, suggestive of an S-phase cell. Late G_1-phase cells have started to spread out on the glass surface but retain the single centromere distribution and with it, dispersed BRCA1 distribution (Fig. 4*J, top*). Again, the larger cell pair in the same figure has BRCA1 accumulations and aggregated centromeres. Large cell pairs with double centromeres are considered cells in the G_2 phase of the cell cycle, and they largely have no BRCA1 accumulations (Fig. 4*K*). We have, however, found large cells with a considerable amount of highly aggregated BRCA1. Most of these cells may be polyploid, *i.e.*, going through nuclear cycles of replication without cytokinesis. The changes in BRCA1 distribution correlate with cell size and centromere distribution and are therefore cell cycle dependent.

Correlation of BRCA1 Localization with Other Nuclear Structures. Because the nucleus appears to be highly compartmentalized, we tested whether BRCA1 accumulations might colocalize with any of the known nuclear compartments. Triple labeling was used to observe the relative location of BRCA1 with the SC35 and ND10 domains. We found that BRCA1 accumulations are largely excluded from the SC35 domains and ND10 (Fig. 5*A*; the yellow appearance of some of the juxtapositions is due to the fortuitous overlap of these domains). In this context, it is remarkable that ND10 is to a large extent situated adjacent to the SC35 domain, whereas only a small fraction of the BRCA1 accumulations abut any of these structures. It is likely that those that do are fortuitously abutting without any functional significance.

The nuclear domains labeled by anti-HP1α antibodies (31) has been reported to have a cell cycle-associated distribution (47). When cells were double labeled for BRCA1 and HP1α, we found three distribution patterns, as illustrated in adjacent cells in Fig. 5*B*. In the middle and smallest cell, sizable accumulations of HP1α, but not BRCA1, are seen. The cell to the right shows several BRCA1 and HP1α accumulations that are mostly separated. However, in the cell nucleus to the left, both antigens seem to be largely overlapping. This finding suggests that BRCA1 overlaps (colocalizes with) HP1α only in a specific part of the cell cycle, most probably during S phase.

Because we had observed only very few cells with BRCA1 accumulations juxtaposed to ND10 and that these accumulations were usually rather large, we asked whether we could force more to this nuclear structure through the overexpression of BRCA1. When cells were transfected with the BRCA1 cDNA transcribed by the cytomegalovirus promoter and probed 16 h after transfection, we found all of the very large BRCA1 accumulations in close association with ND10 (Fig. 5*C*). These BRCA1 aggregations had a near circular outline, contrary to the more irregular outline of the endogenous large BRCA1 accumulations we occasionally found (Fig. 5*D*; the nucleus is outlined in blue by staining for DNA). High BRCA1 aggregations are therefore associated with a specific nuclear domain, ND10. Surprisingly, large amounts of endogenous, as well as overexpressed, BRCA1 accumulated only at a limited number of ND10 and was not equally divided among the ND10, as expected for a protein transported into the nucleus through randomly positioned pore complexes. Therefore, we tested several proteins (that had been reported to associate with ND10) as to whether they where present at only a limited number of ND10 and whether they might be attracting the excess BRCA1. The ubiquitin-specific protease, HAUSP, (48) was the only protein that showed a limited association with ND10 (Fig. 5*E*). However, its distribution and accumulation did not overlap with that of BRCA1 (data not shown).

Effect of Virus Infection on the BRCA1 Distribution. HAUSP has been characterized through its binding to the HSV1 immediate-early protein ICP0 (48). Because we could not find a direct binding of HAUSP with BRCA1, we asked whether the herpesvirus immediate-early protein ICP0, a transactivator that binds to HAUSP and disperses it from its high accumulations at some ND10, would also disperse the
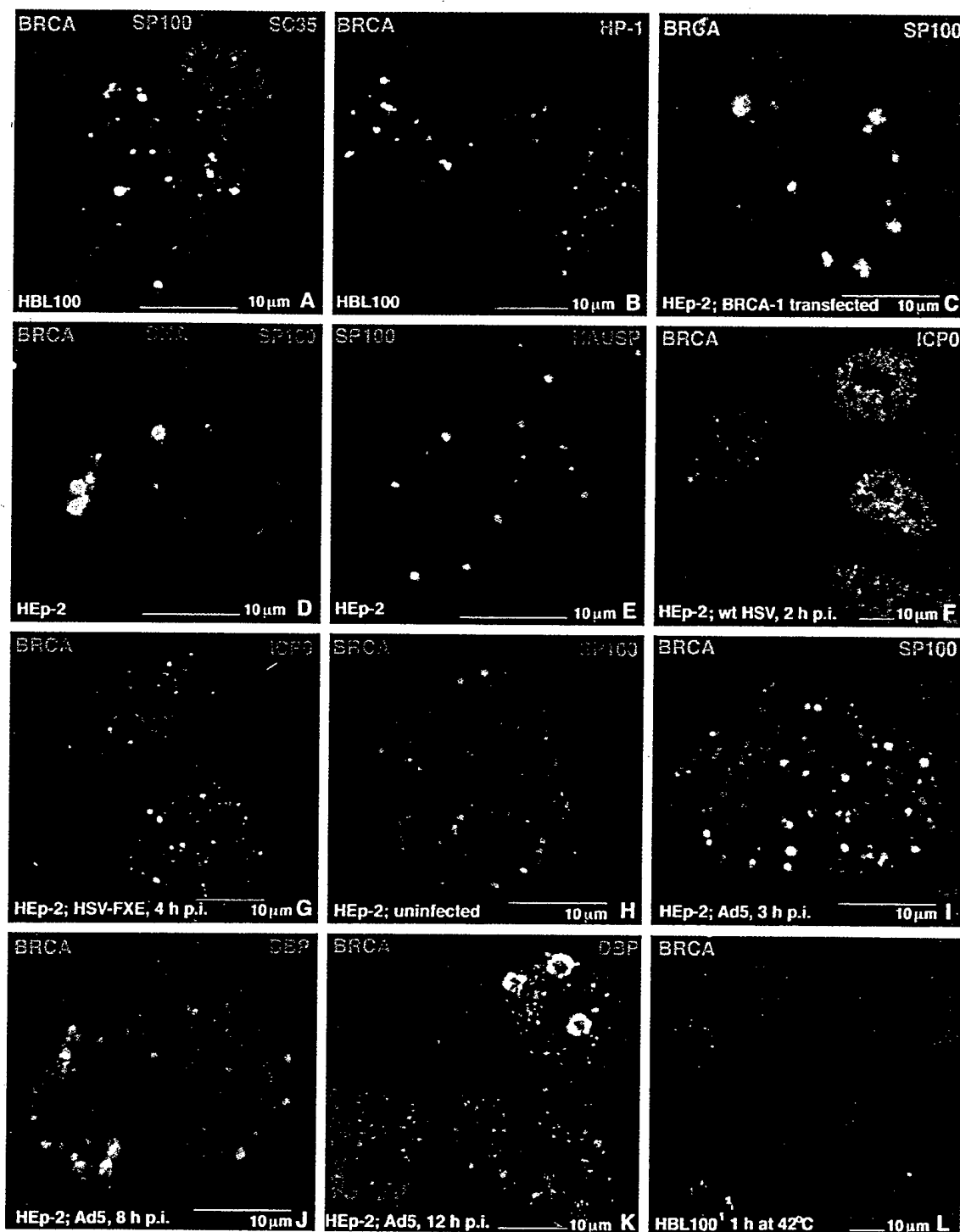
Fig. 5. BRCA1 distribution in relation to other nuclear domains and after virus infection. *A*, triple labeling of HBL100 cells showing that BRCA1 staining does not colocalize with SC35 domains and ND10. *B*, double labeling of HBL100 cells showing that HP-1 may or may not colocalize with BRCA1. *C*, BRCA1-transfected HEp-2 cell showing that overexpressed BRCA1 localizes adjacent to a few ND10. *D*, HEp-2 cell showing high concentrations of endogenous BRCA1 at ND10. *E*, HEp-2 cell double labeled to show that HAUSP localizes adjacent to only a few ND10. *F*, HEp-2 cells 2 h.p.i. with wild-type HSV-1. Cells are double labeled for ICP0 to show which cells are infected and for BRCA1, demonstrating that BRCA1 is dispersed in infected cells. *G*, same as *A* but infected with the RING finger mutant FXE of HSV-1, indicating that infection with this mutant does not disperse BRCA1. *H*, uninfected HEp-2 cells showing the normal distribution of BRCA1 relative to ND10. *I*, HEp-2 cells 3 h.p.i. with Ad5 and stained for BRCA1 and SP100, indicating that SP100 has been distributed to short tracks and BRCA1 is located at many of these tracks. *J*, HEp-2 cells 8 h.p.i. with Ad5 and stained to show the single-stranded DNA binding protein DBP as an indicator where Ad5 replication begins and demonstrating that BRCA1 localizes adjacent to the replication domains. *K*, HEp-2 cells 12 h.p.i. with Ad5, double-labeled for DBP and BRCA1, indicating that BRCA1 localizes to the outer rim of the replication compartment (*upper right*) and is absent from the replication compartment at later stages of the replication cycle (*lower left*). *L*. HBL100 cells stressed for 1 h at 42°C and labeled for BRCA1. All BRCA1 accumulations have dispersed. Optical sections are ~0.7 μm thick

high accumulations of BRCA1 from ND10. We infected cells with wild-type HSV1 for 2 h. All infected cells could be identified by antibodies to the viral protein ICP0, and those so identified had only dispersed BRCA1 throughout the nucleus, whereas uninfected cells showed the expected BRCA1 accumulations (Fig. 5F). This finding shows only that wild-type HSV1 infection disperses BRCA1 accumulations but provides the assay with which to test whether mutations in ICP0 would retain BRCA1 accumulations. When cells were infected with an ICP0 mutant, FXE (where the RING finger region of ICP0 has been deleted), BRCA1 accumulations were retained (Fig. 5G). Thus, the dispersion of BRCA1 in S-phase nuclei by ICP0 represents a new effect of this viral transactivator on a cellular protein.

Ad5 also contains a protein (E4 ORF3) that modifies the location of HAUSP and ND10-associated proteins (39–41). We tested this virus early effect on BRCA1 distribution using the breast cancer cell line HBL100. In uninfected cells, BRCA1 and ND10 are largely positioned in separate domains (Fig. 5H). However, 3 h after infection, ND10 proteins were redistributed into many short tracks, and BRCA1 was now found in association with these tracks (Fig. 5I). Previously, we had shown by in situ hybridization that Ad5 replicates at sites where the viral single-stranded DNA protein, DBP, accumulates (41). At these later stages (8 h.p.i.), we found BRCA1 juxtaposed to replication domains (Fig. 5J). When these Ad5 replication domains expand, BRCA1 was recruited to these domains and surrounded them (Fig. 5K). When viral replication advanced further, as indicated by the accumulation of DBP throughout much of the nucleus, BRCA1 is no longer detected around these sites but only in those nuclear spaces where no viral accumulation is evident (left lower cell in Fig. 5K). Finding BRCA1 to be recruited to the outside of the viral replication domain where transcription of this virus takes place suggests that the virus makes use of this cellular protein in its transcriptional processes.

To test this hypothesis, we disturbed the global transcriptional processes through stress, which acts by shutting down normal transcription or processing and activating the transcription of the heat shock proteins (49–52). Such a global change may then either change BRCA1 distribution to: (a) a dispersed state in all cells; or (b) an accumulated state in all cells. When we treated HEp-2 cells for 1 h at 42°C, all BRCA1 accumulations were dispersed, with the BRCA1 distribution appearing as in cells in the G_1-phase of the cell cycle. BRCA1 distribution therefore changes in response to stress (heat shock) as well as to DNA-damaging agents (10, 53).

Discussion

Investigations of the molecular interactions of BRCA1 are progressing at several fronts, but knowledge of supramolecular events involving BRCA1 is largely absent. In this report, we have, therefore, begun to evaluate the distribution of BRCA1 at the cellular level during the cell cycle, determined its potential interactions at various nuclear domains, and have started to define its behavior in response to external stimuli, such as stress and viral infection. To embark on this work required antibodies that could be relied upon to visualize the location of BRCA1. Previously, BRCA1 had

been shown to localize to the cell membrane and was considered a secreted protein (12). This localization has since been shown to be due to the cross-reactivity of the C20 antibody to the EGF receptor (53, 54). We therefore produced a MAb (BR64) that recognizes the native antigen as well as BRCA1 expressed after transfection of various expression plasmids. When compared with other anti-BRCA1 MAbs, the MAb BR64 showed equivalent nuclear distribution but also reacted with a cytoplasmic component, the centrosome. The same reactivity was found for other BRCA1 MAbs and the polyclonal antibody C20. Although the centrosome reactivity of all these antibodies may be a cross-reactivity, the fact that the antibodies were made against quite different epitopes argues against this interpretation. We therefore consider that this result is suggestive of BRCA1 binding to this cellular domain so intimately involved in mitotic events. Furthermore, our use of BR64 hybridoma supernatant excludes the possibility of a contaminating mouse autoantibody. The reaction of C-20 with the Flemming body, however, may be such an autoantibody present in rabbits. The least useful MAb for our analyses was 17F8, because it cross-reacted with a number of cytoplasmic granules. Furthermore, because of the thickness of the optical section (~0.7 μm), these granules overlaid the nuclear domain and did not allow for an unbiased determination of the nuclear distribution of BRCA1. The cross-reactivity of M13 with cytoplasmic filaments made this antibody useful only for cells without these filaments. We had observed, however, that even HEp-2 cells in mitosis had the cytoplasmic dot characteristic of depolymerized intermediate filaments. The faint cytoplasmic staining in HEp-2 cells may therefore be due to a low level of these filaments. The general conclusions of the comparison of the different BRCA1 antibodies is that: (a) they collectively validate the presence of BRCA1 in the nucleus; and (b) they can be used to evaluate the redistribution of BRCA1 induced by internal physiological changes and externally induced effects, but only in cells where the cross-reactive proteins are absent.

For all antibodies, we had observed two distribution patterns for BRCA1, dispersed and aggregated. That smaller cells had only dispersed BRCA1 suggested a cell cycle-related event. A general interruption of the cell cycle is possible through the application of stress in the form of heat shock. Cellular transcription and splicing is reduced and shifted to heat shock protein transcription. Under these conditions, BRCA1 becomes dispersed from its domains, similar to other proteins resident in other domains. Whether this phenomenon can be attributed to a change in transcription or to the subsequent cell cycle retardation is not clear, but it presents a new single-cell assay of an as-yet-to-be defined BRCA1 function.

There are no precise cell cycle markers that can be used in a single-cell assay such as microscopy, particularly because the BRCA1 epitopes seem to be sensitive to the acid treatment necessary to expose the S-phase indicator bromodeoxyuridine.[4] However, He and Brinkley (46) showed that cen-

---

[4] G. Maul, unpublished results.

tromeres behave quite predictably during the cell cycle. The dispersion of the centromeres after mitosis lasts into later parts of G_1 and was correlated with dispersed states of BRCA1. The centromeres aggregated later, and the numbers that can be counted are far below those expected for the number of chromosomes present. This stage corresponds, according to He and Brinkley (46), to the S-phase and is clearly correlated with the presence of aggregated BRCA1. At the end of the cell cycle, cells are rather large, and the centromeres are present as pairs and are not highly clustered. The distribution pattern of BRCA1 in large cells is less clear, but the bulk of those observed (which had paired centromeres) also had few or no sites of aggregated BRCA1. From these observations, it is clear that BRCA1 changes its distribution during the cell cycle and that aggregation is predominantly present during the S-phase of the cell cycle, with a more precise definition of this phenomenon not presently possible. Arising from these observations is the question of whether the areas of accumulation define the sites of active BRCA1, or whether, alternatively, BRCA1 may act in the "dispersed" mode with the "aggregated" state being sites of storage for BRCA1 (segregation).

The nucleus is partitioned into domains of various activities. Not only do specific chromosomal territories exist (55), but so do various extrachromosomal domains to which specific functions are attributable and which can be delineated with the respective antibodies. We did not find any domain that consistently colocalized with BRCA1. BRCA1 accumulations definitely reside outside of the SC35 domain and the ND10. However, BRCA1 accumulations overlap HP1α during a stage of S phase. PIKA represent domains of highly aggregated HP1α, a protein that is normally associated with heterochromatin (47). HP1α has also been shown to change its aggregation pattern during the S-phase of the cell cycle (47). Contrary to BRCA1, however, it starts in a highly aggregated, BRCA1-sized domain, during G_1. The temporary association of the two proteins in the same nuclear domain does not necessarily signify direct interaction, a conclusion supported by a two-hybrid assay in which no interaction could be found.[4] Other proteins may be intermediaries; however, these two proteins are the only ones presently showing cell cycle-dependent colocalization.

The accumulation of a protein may be viewed as indicative of: (a) functioning at this site; (b) as segregation with the implication of removing the protein from functioning; or (c) storing excess protein as a means to regulate the precise amount of protein in a delicate balance. This balance may change during the cell cycle. Under these assumptions, we may either conclude that BRCA1 has specific nuclear sites of high activity during S phase, or its concentration throughout the nucleus is lowered by segregation during this part of the cell cycle. The possibility that the cell has the capability to segregate endogenous BRCA1 is supported by the finding of high concentrations close to ND10 and the accumulation of BRCA1 at these sites when overexpressed. We may be witnessing segregation of BRCA1 into a nuclear dump or nuclear depot (56).

Viruses have often been instrumental in the elucidation of cellular functions. Using two DNA viruses we could demonstrate that they modify BRCA1 distribution quite differently and provide a single-cell assay to test this perturbation. The dispersion of BRCA1 by HSV1 may be due to the interruption of the cell cycle as HSV1 blocks S phase (57). However, we were able to define the immediate-early HSV1 *IE1* gene as an essential gene for BRCA1 dispersion. Its potential interaction with a BRCA1 pathway may lay at the center of the inability of cells to grow when ICP0 is constitutively expressed.[4]

Ad5 has a quite different effect on BRCA1. BRCA1 accumulates at and surrounds some of the replication sites during the viral replication. Later, after transcription and replication cease late in the replication cycle, BRCA1 is no longer present around the viral replication domain as indicated by staining against DBP. The outer fringe of the replication site represents viral single-stranded DNA that is being transcribed, whereas the center contains double-stranded Ad5 DNA (58). The presence of BRCA1 at the outer region of Ad5 suggests that it may be used in viral transcription. Alternatively, because this outer region is also where decatenation of the viral DNA takes place, BRCA1 accumulation in this area may suggest a role in this process, a role supported by the observation that BRCA1 may be involved in the crossover mechanism during pachyteen of meiosis (6).

This investigation establishes that there is a cell cycle-related change in the distribution of BRCA1 in the nucleus and that another protein, HP1, involved in transcriptionally silencing chromatin, colocalizes during part of BRCA1 accumulation/segregation. We found that DNA viruses change the distribution of BRCA1 substantially and, in the case of Ad5, temporarily recruit this protein into an area of high transcriptional activity.

Materials and Methods

Cell Culture. All cells were maintained at 37°C and 5% CO_2. MCF7 cells (ATCC HTB 22) and HBL-100 (ATCC HTB 124) cells were grown in high glucose DMEM containing 10% FBS and 0.1 mM nonessential amino acids. MDA-MB-468 (ATCC HTB 132) cells were grown in a 1:1 mix of high glucose DMEM and Ham's F-12 with 10% FBS. Human WI38 fibroblasts (ATCC CCL 75) and the epithelial cell line HEp-2 (ATCC CCL 23) were maintained in MEM supplemented with 10% FCS and antibiotics.

$^{32}PO_4$ Labeling of MDA-MB-468 Cells. MDA-MB-468 cells were rinsed twice with warm, phosphate-free DMEM (hi glucose) medium and then incubated in phosphate-free medium containing 5% dialyzed FBS for 2 h. The cells were then placed in phosphate-free medium containing 5% dialyzed FBS and $^{32}PO_4$ (100 μCi/ml; NEN) and incubated for an additional 2 h. Cells were harvested in RIPA buffer containing 50 mM NaF and protease inhibitors [20 mM HEPES (pH 7.4), 140 mM NaCl, 1% Triton X-100, 1% deoxycholate, 0.1% SDS, 1 mM EDTA, 1 mM phenylmethyl-sulfonyl fluoride, 2 μg/ml leupeptin, 0.04 TI units/ml aprotinin, and 2 μg/ml pepstatin].

MAb Production. A synthetic gene of the BRCA1-RF domain (amino acids 1–100) was made from overlapping oligonucleotides whose codon usage had been optimized for expression in *E. coli* and *Saccharomyces cerevisiae* (5, 59). Double-stranded DNA was generated by the PCR. This BRCA1 partial cDNA was fused downstream of the six His residues of the vector pQE-30 (Qiagen, Inc.). The His-tagged protein was purified from *E. coli* over a nickel-agarose column as described previously (20). Fifty μg of recombinant 6XHis-BRCA1 fusion protein, in 50 μl PBS, was emulsified in complete Freund adjuvant and injected s.c. into BALB/c mice, followed by three boosts in incomplete Freund adjuvant. The fourth boost was given i.v., and the splenocytes were fused 3 days later with the mouse nonimmunoglobulin-secreting cell line P3X63Ag8.SP2/0. Hybridomas were selected by testing supernatants by ELISA on recombinant 6XHis-BRCA1.

Each clone was subcloned following standard procedures. All resulting MAbs were of IgG1, kappa.

Immunoprecipitations. Immunoprecipitation of samples with polyclonal Abs was performed with protein A-Sepharose (Pharmacia). The MAb BR64 was precipitated with protein G-Sepharose (Pharmacia). Immunoprecipitations were carried out by incubating the antibody with protein extract or in vitro-produced protein in 1 ml of RIPA buffer for 2 h at 4°C. The protein G (or A) Sepharose resin was then added, and the reaction incubated an additional 30–45 min at 4°C with continual mixing. The bound proteins were washed in RIPA buffer five times, released from the Sepharose resin with SDS-PAGE loading dye, and separated by SDS-PAGE. Visualization of bound protein was performed by autoradiography.

Western Blot Analysis. Proteins were separated by SDS-PAGE and transferred to PVDF membrane (Millipore) via standard methods. In Fig. 2B, the membrane was blocked in Tris-buffered saline containing 0.1% Tween-20 (TBST) and 5% fish gelatin (Forma Scientific). The MAb BR64 ascites fluid was diluted 1:1000 in the block buffer and incubated with the membrane for 2 h at room temperature with gentle shaking. After washing the membrane five times with TBST (10 min each), the blot was incubated with secondary antibody conjugated to horseradish peroxidase (goat anti-mouse IgG-HRP; Bio-Rad) at 1:5000 dilution for 30 min. The membrane was washed five times further and developed with Super Signal (Pierce). In Fig. 2C, the membrane was blocked for 1 h in Tris-buffered saline containing 0.2% Tween-20 (TBST2) and 5% dry milk. The MAb BR64 ascites fluid was diluted to 0.5 µg/ml (TBST2 plus 1% BSA) and incubated with the membrane for 1 h at room temperature with gentle shaking. After washing the membrane three times with TBST2 (10 min each), the blot was incubated with secondary antibody conjugated to alkaline phosphatase (alkaline phosphatase anti-mouse IgG; Promega) at 1:7500 dilution (TBST2 plus 1% BSA) for 45 min. The membrane was washed three times further and developed using 5-bromo-4-chloro-3-indolyl phosphate/nitroblue tetrazolium color development substrates (Promega).

Transfections and in Vitro Transcription/Translation. Cells were transiently transfected by calcium phosphate precipitation (60). The Promega TNT kit was used as described by the manufacturer to produce 35S-labeled protein. Proteins were used for analysis without further purification. Plasmid constructs bearing BRCA1 and BRCA1-Δ11 were kind gifts of F. Calzone (Amgen, Inc., Thousand Oaks, CA). The RPT-1 cDNA was a kind gift of H. Cantor (Dana-Farber Cancer Institute, Boston, MA) (44).

Antibodies Used for Immunofluorescence. Antibodies used for the detection of BRCA1 were: M13, a MAb kindly provided by R. Scully (Dana-Farber Cancer Institute, Boston, MA) (61); 17F8, a MAb kindly provided by W. H. Lee (Center for Molecular Medicine, University of Texas Health Science Center, San Antonio, TX) (11); and C20, a rabbit polyclonal antibody that was purchased from Santa Cruz Biotechnologies (Palo Alto, CA).

ND10 were visualized using MAb 1150, which recognizes Sp100 (62). The human antibody 1745, which recognizes Sp100 and PML, was used in triple-labeling experiments (62). MAb anti-SC35 (25) was used to label the SC35 domain. MAbs against HAUSP and ICP0 were provided by R. Everett (Medical Research Council, Glasgow, UK) (48). Isotype-matched MAbs of unrelated specificity served as controls. Rabbit anti-HP1α antibodies were obtained from W. Earnshaw (University of Edinburgh, Ediburgh, UK) (31).

Immunohistochemistry. Cells were fixed at room temperature for 15 min with freshly prepared 1% paraformaldehyde in PBS, washed with PBS, and permeabilized for 20 min on ice with 0.2% (v/v) Triton X-100 (Sigma Chemical Co.) in PBS. Antigen localization was determined after incubation of permeabilized cells with rabbit antiserum, MAb, or human antiserum diluted in PBS for 1 h at room temperature. Avidin-fluorescein or avidin-Texas Red was complexed with primary antibodies through biotinylated secondary antibodies (Vector Laboratories). Cells were double- or triple-labeled with the respective second antibodies conjugated with FITC, Texas Red, or Cy-5 using biotin-avidin enhancement and FITC for structures with the lowest staining intensity. Cells were then stained for DNA with 0.5 µg/ml of bis-benzimide (Hoechst 33258; Sigma) in PBS and mounted with Fluoromount G (Fisher Scientific). Cells were analyzed using a Leica confocal scanning microscope. The two channels were recorded simultaneously when no cross-talk was detectable. In the case of intense

FITC-labeling, sequential images were acquired with more restrictive filters to prevent possible breakthrough of the FITC signal into the red channel. Both acquisition modes gave the same results. Leica image enhancement software was used in balancing signal strength. Because of the variability of the infectious cycle progression in any given culture, the most prevalent and representative images were photographed and presented as a limited number of nuclear images to retain high magnification. At least 500 cells were studied in each sample.

Virus Infection. Two days after plating, HEp-2 cells were infected with HSV-1 17⁻ at 2 plaque-forming units/cell, resulting in 95% infected cells as determined by staining for ICP0 antibodies at 5 h.p.i. Cells were fixed at different intervals after infection and assayed with different antibodies as described (34). Ad5 infection was carried out as described (41), and cells were fixed at various times after infection.

References

1. Miki, Y., Swensen, J., Shattuck-Eidens, D., Futreal, P. A., Harshman, K., Tavtigian, S., Liu, Q., Cochran, C., Bennett, L. M., Ding, W., et al. A strong candidate for the breast and ovarian cancer susceptibility gene BRCA1. Science (Washington DC), 266: 66–71, 1994.

2. Chen, C. F., Li, S., Chen, Y., Chen, P. L., Sharp, Z. D., and Lee, W. H. The nuclear localization sequences of the BRCA1 protein interact with the importin-α subunit of the nuclear transport signal receptor. J. Biol. Chem., 271: 32863–32868, 1996.

3. Wu, L. C., Wang, Z. W., Tsan, J. T., Spillman, M. A., Phung, A., Xu, X. L., Yang, M. C., Hwang, L. Y., Bowcock, A. M., and Baer, R. Identification of a RING protein that can interact in vivo with the BRCA1 gene product. Nat. Genet., 14: 430–440, 1996.

4. Jin, Y., Xu, X. L., Yang, M-C. W., Wei, F., Ayi, T-C., Bowcock, A. M., and Baer, R. Cell cycle-dependent colocalization of BARD1 and BRCA1 proteins in discrete nuclear domains. Proc. Natl. Acad. Sci. USA, 94: 12075–12080, 1997.

5. Jensen, D. E., Proctor, M., Marquis, S. T., Gardner, H. P., Ha, S. I., Chodosh, L. A., Ishov, A. M., Tommerup, N., Vissing, H., Sekido, Y., Minna, J., Borodovsky, A., Schultz, D. C., Wilkinson, K. D., Maul, G. G., Barlev, N., Berger, S. L., Prendergast, G. C., and Rauscher, F. J., III. BAP1: a novel ubiquitin hydrolase which binds to the BRCA1 RING finger and enhances BRCA1-mediated cell growth suppression. Oncogene, 16: 1097–1112, 1998.

6. Thompson, M. E., Jensen, R. A., Obermiller, P. S., Page, D. L., and Holt, J. T. Decreased expression of BRCA1 accelerates growth and is often present during sporadic breast cancer progression. Nat. Genet., 9: 444–450, 1995.

7. Rao, V. N., Shao, N., Ahmak, M., and Reddy, E. S. P. Antisense RNA to the putative tumor suppressor gene BRCA1 transforms mouse fibroblasts. Oncogene, 12: 523–528, 1996.

8. Holt, J. T., Thompson, M. E., Szabo, C., Robinson-Benion, C., Arteaga, C. L., King, M-C., and Jensen, R. A. Growth retardation and tumour inhibition by BRCA1. Nat. Genet., 12: 298–302, 1996.

9. Scully, R., Chen, J., Plug, A., Xiao, Y., Weaver, D., Feunteun, J., Ashley, T., and Livingston, D. M. Association of BRCA1 with Rad51 in mitotic and meiotic cells. Cell, 88: 265–275, 1997.

10. Scully, R., Chen, J., Ochs, R. L., Keegan, K., Hoekstra, M., Feunteun, J., and Livingston, D. M. Dynamic changes of BRCA1 subnuclear location

and phosphorylation state are initiated by DNA damage. Cell. *90:* 425–435. 1997.

11. Chen. Y., Chen. C. F., Riley. D. J.. Allred, D. C.. Chen, P. L., Von Hoff, D., Osborne. C. K.. and Lee, W. H. Aberrant subcellular localization of BRCA1 in breast cancer. Science (Washington DC). *270:* 789–791. 1995.

12. Jensen. R. A., Thompson, M. E.. Jetton, T. L.. Szabo. C. I., van der Meer, R., Helou, B.. Tronick. S. R.. Page. D. L.. King. M-C. and Holt. J. T. BRCA1 is secreted and exhibits properties of a granin. Nat. Genet.. *12:* 303–308. 1996.

13. Koonin. E. V., Altschul, S. F., and Bork, P. BRCA1 protein products. Functional motifs. Nat. Genet., *13:* 266–268, 1996.

14. Chapman, M. S., and Verma, I. M. Transcriptional activation by BRCA1. Nature (Lond.). *382:* 678–679, 1996.

15. Scully, R., Anderson, S. F., Chao, D. M., Wei, W.. Ye. L., Young. R. A., Livingston. D. M., and Parvin. J. D. BRCA1 is a component of the RNA polymerase II holoenzyme. Proc. Natl. Acad. Sci. USA. *94:* 5605–5610. 1997.

16. Borden, K. L., Boddy, M. N., Lally. J.. O'Reilly, N. J., Martin. S., Howe, K., Solomon, E., and Freemont, P. S. The solution structure of the RING finger domain from the acute promyelocytic leukaemia proto-oncoprotein PML. EMBO J., *14:* 1532–1541, 1995.

17. Lovering. R., Hanson, I. M., Borden, K. L., Martin, S., O'Reilly, N. J., Evan, G. I., Rahman, D., Pappin, D. J., Trowsdale, J., and Freemont, P. S. Identification and preliminary characterization of a protein motif related to the zinc finger. Proc. Natl. Acad. Sci. USA. *90:* 2112–2116, 1993.

18. Klug. A., and Schwabe, J. W. Protein motifs 5. Zinc fingers. FASEB J., *9:* 597–604, 1995.

19. Saurin. A. J., Borden, K. L. B., Boddy, M. N., and Freemont, P. S. Does this have a familiar RING? Trends Biochem. Sci., *21:* 208–214, 1996.

20. Friedman, J. R., Fredericks, W. J., Jensen, D. E., Speicher, D. W., Huang, X. P., Neilson, E. G., and Rauscher, F. J. R. KAP-1, a novel corepressor for the highly conserved KRAB repression domain. Genes Dev., *10:* 2067–2078, 1996.

21. Gudas, J. M., Nguyen, H., Li, T., and Cowan, K. H. Hormone-dependent regulation of BRCA1 in human breast cancer cells. Cancer Res., *55:* 4561–4565. 1995.

22. Gudas, J. M., Tao, L., Nguyen, H., Jensen, D., Rauscher, F. J., III, and Cowan, K. H. Cell cycle regulation of BRCA1 messenger RNA in human breast epithelial cells. Cell Growth Differ.. *7:* 717–723. 1996.

23. Vaughn, J. P.. Davis. P. L., Jarboe. M. D., Huper. G., Evans, A. C., Wiseman, R. W., Berchuck. A., Iglehart. J. D., Futreal. A.. and Marks. J. R. BRCA1 expression is induced before DNA synthesis in both normal and tumor-derived breast cells. Cell Growth Differ., *7:* 711–715. 1996.

24. Marks. J. R., Huper. G., Vaughn. J. P.. Davis. P. L., Norris. J., McDonnell. D. P.. Wiseman. R. W.. Futreal. P. A.. and Iglehart. J. D. BRCA1 expression is not directly responsive to estrogen. Oncogene, *14:* 115–121, 1997.

25. Fu, X. D.. and Maniatis. T. Factor required for mammalian spliceosome assembly is localized to discrete regions in the nucleus. Nature (Lond.). *343:* 437–441. 1990.

26. Spector. D. L.. Fu, X. D.. and Maniatis. T. Associations between distinct pre-mRNA splicing components and the cell nucleus. EMBO J.. *10:* 3467–3481. 1991.

27. Carmo-Fonseca. M.. Pepperkok. R., Carvalho, M. T.. and Lamond. A. I. Transcription-dependent colocalization of the U1. U2. U4/U6. and U5 snRNPs in coiled bodies. J. Cell Biol.. *117:* 1–14. 1992.

28. Frey. M. R., and Matera. A. G. Coiled bodies contain U7 small nuclear RNA and associate with specific DNA sequences in interphase human cells [published erratum appears in Proc. Natl. Acad. Sci. USA, *92:* 8532. 1995]. Proc. Natl. Acad. Sci. USA, *92:* 5915–5919. 1995.

29. Smith. K. P., Carter, K. C., Johnson. C. V.. and Lawrence. J. B. U2 and U1 snRNA gene loci associate with coiled bodies. J. Cell. Biochem.. *59:* 473–485. 1995.

30. Gao. L.. Frey. M. R.. and Matera. A. G. Human genes encoding U3 snRNA associate with coiled bodies in interphase cells and are clustered on chromosome 17p11.2 in a complex inverted repeat structure. Nucleic Acids Res.. *25:* 4740–4747. 1997.

31. Saunders. W. S., Cooke. C. A.. and Earnshaw. W. C. Compartmentalization within the nucleus: discovery of a novel subnuclear region. J. Cell Biol., *115:* 919–931. 1991.

32. Dyck, J. A.. Maul. G. G., Miller. W. H.. Jr.. Chen. J. D., Kakizuka. A., and Evans, R. M. A novel macromolecular structure is a target of the promyelocyte-retinoic acid receptor oncoprotein. Cell, *76:* 333–343. 1994.

33. Desbois. C.. Rousset, R., Bantignies, F.. and Jalinot, P. Exclusion of Int-6 from PML nuclear bodies by binding to the HTLV-I Tax oncoprotein. Science (Washington DC). *273:* 951–953. 1996.

34. Maul. G. G.. Ishov, A. M., and Everett. R. D. Nuclear domain 10 as preexisting potential replication start sites of herpes simplex virus type-1. Virology. *217:* 67–75, 1996.

35. Ishov. A. M.. Stenberg. R. M., and Maul. G. G. Human cytomegalovirus immediate early interaction with host nuclear structures: definition of an immediate transcript environment. J. Cell Biol.. *138:* 5–16, 1997.

36. Maul, G. G.. Guldner. H. H., and Spivack. J. G. Modification of discrete nuclear domains induced by herpes simplex virus type 1 immediate early gene 1 product (ICP0). J. Gen. Virol., *74:* 2679–2690, 1993.

37. Maul. G. G., and Everett. R. D. The nuclear location of PML, a cellular member of the C3HC4 zinc-binding domain protein family, is rearranged during herpes simplex virus infection by the C3HC4 viral protein ICP0. J. Gen. Virol., *75:* 1223–1233. 1994.

38. Everett. R. D., and Maul. G. G. HSV-1 IE protein Vmw110 causes redistribution of PML. EMBO J.. *13:* 5062–5069, 1994.

39. Carvalho. T.. Seeler, J. S., Ohman, K., Jordan, P., Pettersson, U., Akusjarvi, G., Carmo-Fonseca, M., and Dejean. A. Targeting of adenovirus E1A and E4-ORF3 proteins to nuclear matrix-associated PML bodies. J. Cell Biol., *131:* 45–56, 1995.

40. Doucas, V.. Ishov. A. M., Romo. A., Juguilon, H., Weitzman, M. D., Evans, R. M., and Maul. G. G. Adenovirus replication is coupled with the dynamic properties of the PML nuclear structure. Genes Dev., *10:* 196–207, 1996.

41. Ishov, A. M., and Maul, G. G. The periphery of nuclear domain 10 (ND10) as site of DNA virus deposition. J. Cell Biol., *134:* 815–826. 1996.

42. Thakur, S., Zhang. H. B., Peng, Y., Le, H.. Carroll, B.. Ward, T., Yao, J., Farid, L. M.. Couch, F. J., Wilson. R. B., and Weber, B. L. Localization of BRCA1 and a splice variant identifies the nuclear localization signal. Mol. Cell. Biol.. *17:* 444–452, 1997.

43. Hogervorst, F. B.. Cornelis, R. S.. Bout. M., van Vliet, M., Oosterwijk, J. C., Olmer. R.. Bakker, B., Klijn. J. G., Vasen. H. F., Meijers-Heijboer. H., et al. Rapid detection of BRCA1 mutations by the protein truncation test. Nat. Genet.. *10:* 208–212, 1995.

44. Patarca, R.. Freeman, G. J.. Schwartz. J.. Singh, R. P., Kong. Q. T., Murphy, E., Anderson, Y., Sheng. F. Y., Singh, P.. Johnson, K. A., et al. rpt-1, an intracellular protein from helper/inducer T cells that regulates gene expression of interleukin 2 receptor and human immunodeficiency virus type 1. Proc. Natl. Acad. Sci. USA, *85:* 2733–2737, 1988.

45. Chen. Y.. Farmer, A. A., Chen. C. F., Jones. D. C., Chen, P. L., and Lee, W. H. BRCA1 is a 220-kDa nuclear phosphoprotein that is expressed and phosphorylated in a cell cycle-dependent manner. Cancer Res., *56:* 3168–3172, 1996.

46. He, D., and Brinkley, B. R. Structure and dynamic organization of centromeres/prekinetochores in the nucleus of mammalian cells. J. Cell Sci., *109:* 2693–2704, 1996.

47. Saunders. W. S., Chue, C.. Goebl, M., Craig. C., Clark, R. F., Powers. J. A., Eissenberg. J. C.. Elgin. S. C.. Rothfield, N. F., and Earnshaw, W. C. Molecular cloning of a human homologue of Drosophila heterochromatin protein HP1 using anti-centromere autoantibodies with anti-chromo specificity. J. Cell Sci.. *104:* 573–582, 1993.

48. Everett. R. D.. Meredith, M., Orr, A.. Cross. A., Kathoria, M.. and Parkinson. J. A novel ubiquitin-specific protease is dynamically associated with the PML nuclear domain and binds to a herpesvirus regulatory protein. EMBO J.. *16:* 1519–1530, 1997.

49. Sadis. S.. Hickey, E., and Weber, L. A. Effect of heat shock on RNA metabolism in HeLa cells. J. Cell. Physiol.. *135:* 377–386. 1988.

50. Utans. U.. Behrens. S. E.. Luhrmann. R.. Kole, R.. and Kramer, A. A splicing factor that is inactivated during in vivo heat shock is functionally equivalent to the {U4·U6·U5} triple snRNP-specific proteins. Genes Dev.. 6: 631–641. 1992.

51. Bond. U. Heat shock but not other stress inducers leads to the disruption of a subset of snRNPs and of in vitro splicing in HeLa cells [published errata appears in E⋯ ⋯020. 1988]. EMBO J.. 7: 3509–3518. 1988.

52. Yost, H. J.. and Lindquist. S. RNA splicing is interrupted by heat shock and is rescued by heat shock protein synthesis. Cell. 45: 185–193. 1986.

53. Thomas. J. E.. Smith. M.. Rubinfeld. B.. Gutowski. M.. Beckmann. R. P., and Polakis. P. Subcellular localization and analysis of apparent 180-kDa and 220-kDa proteins of the breast cancer susceptibility gene. BRCA1. J. Biol. Chem.. 271: 28630–28635. 1996.

54. Wilson. C.. Payton. M. N.. Pekar. S⋯ ⋯ng. K., Pacifici, R. E.. Gudas. J. L.. Thukral. S. Calzone. F. J.. F⋯ ⋯M . and Slamon, D. I. BRCA1 protein produ⋯ ⋯t body specific⋯ ⋯ Genet., 13: 264–265. 1996.

55. Lichter, P.. Cremer ⋯ Borden. J.. Manuelidis, L.. and Ward. ⋯ ⋯ Delineation of individual human chromosomes in metaphase and interphase cells by in situ suppression hybridization using recombinant DNA libraries. Hum. Genet., 80: 224–234, 1988.

56. Maul. G. G. Nuclear domain 10. the site of DNA virus transcription and replication. BioEssay. 20: 660–667. 1998.

57. de Bruyn Kops. A.. and Knipe. D. M. Formation of DNA replication structures in herpes virus-infected cells requires a viral DNA binding ⋯ain. Cell. 55: 857–868. 1988.

58. Thiry. M.. and Puvion-Dutilleul F. Differential distribution of single-stranded DNA. double-stranded DNA. and RNA in adenovirus-induced intranuclear regions of HeLa cells. J. Histochem. Cytochem.. 43: 749–759. 1995.

59. Madden. S. L.. Cook. D. M.. Morris. J. F.. Gashler, A.. Sukhatme. V. P.. and Rauscher, F. J.. III. Transcriptional repression mediated by the WT1 Wilms tumor gene product. Science (Washington DC). 253: 1550–1553, 1991.

60. Chen. C.. and Okayama. H. High-efficiency transformation of mammalian cells by plasmid DNA. Mol. Cell. Biol.. 7: 2745–2752, 1987.

61. S⋯ ⋯ Ganesan. S.. Brown, M.. Caprio. J. A. D.. Cannistra. S. A.. Feunte⋯ Schnitt. S., and Livingston. D. M. Location of BRCA1 in human breast and ovarian cancer cells. Science (Washington DC). 272: 123–126. 1996.

62. Maul. G. G.. Yu. E.. Ishov. A. M.. and Epstein, A. L. Nuclear domain 10 (ND10) associated proteins are also present in nuclear bodies and redistribute to hundreds of nuclear sites after stress. J. Cell. Biochem.. 59: 498–513. 1995.